



Shahid Chamran
University of Ahvaz

Journal of Applied and Computational Mechanics



Research Paper

Theoretical Study on Poiseuille Flow of Herschel-Bulkley Fluid in Porous Media

D.S. Sankar¹, K.K. Viswanathan^{2,3}, Atulya K. Nagar⁴, Nurul Aini Binti Jafaar⁵, A. Vanav Kumar⁶

¹ Applied Mathematics and Economics Programme, School of Applied Sciences and Mathematics, Universiti Teknologi Brunei, Jalan Tungku Link, Bandar Seri Begawan, BE1410, Brunei Darussalam, Email: sankar_ds@yahoo.co.in

² UTM Centre for Industrial and Applied Mathematics, Ibnu Sina Institute for Scientific and Industrial Research, Universiti Teknologi Malaysia, 81310 Johor Bharu, Johor, Malaysia, Email: visu20@yahoo.com

³ Ship & Offshore Extreme Technology Industry-Academic Co-operation Research Center, Inha university, 100 Inha-ro, Incheon, 22212, South Korea

⁴ School of Mathematics, Computer Science and Engineering, Liverpool Hope University, Hope Park, Liverpool L16 9JD, United Kingdom, Email: naragara@hope.ac.uk

⁵ Department of Mathematical Sciences, Universiti Teknologi Malaysia, 81310 Johor Bharu, Johor, Malaysia, Email: nurulaini.jaafar20@utm.my

⁶ Department of Mathematics, National Institute of Technology, Yupia - 791112, Arunachal Pradesh, India, Email: vanavkumar.a@gmail.com

Received March 15 2021; Revised May 30 2021; Accepted for publication May 30 2021.

Corresponding author: D.S. Sankar (sankar_ds@yahoo.co.in)

© 2022 Published by Shahid Chamran University of Ahvaz

Abstract. This theoretical study analyses the effects of geometrical and fluid parameters on the flow metrics in the Hagen-Poiseuille and plane-Poiseuille flows of Herschel-Bulkley fluid through porous medium which is considered as (i) single pipe/single channel and (ii) multi-pipes/multi-channels when the distribution of pores size in the flow medium are represented by each one of the four probability density functions: (i) Uniform distribution, (ii) Linear distribution of Type-I, (iii) Linear distribution of Type-II and (iv) Quadratic distribution. It is found that in Hagen-Poiseuille and plane-Poiseuille flows, Buckingham-Reiner function increases linearly when the pressure gradient increases in the range 1 - 2.5 and then it ascends slowly with the raise of pressure gradient in the range 2.5 - 5. In all of the four kinds of pores size distribution, the fluid's mean velocity, flow medium's porosity and permeability are substantially higher in Hagen-Poiseuille fluid rheology than in plane-Poiseuille fluid rheology and, these flow quantities ascend considerably with the raise of pipe radius/channel width and a reverse characteristic is noted for these rheological measures when the power law index parameter increases. The flow medium's porosity decreases rapidly when the period of the pipes/channels distribution rises from 1 to 2 and it drops very slowly when the period of the pipes/channels rises from 2 to 11.

Keywords: Mathematical analysis; Porous medium; Permeability; Porosity; Mean velocity.

1. Introduction

The rheology of different kinds of fluids in porous media is an upcoming and important rheological phenomena which finds numerous technological applications in various fields viz bio-medical engineering, chemical engineering, petroleum engineering, manufacturing engineering etc. [1 - 3]. Porous media can be found everywhere around us, i.e. they can be found in living things (human skin, digestive systems, blood flow in arterioles), nature (river beds and agricultural fields absorb water), and in various industrial applications such as storage of solar heat energy in granular porous media, storing heat energy for residential houses using phase change material, storing pollutants in porous materials and their usage in certain biological actions, viz membrane transport, dialysis etc. [4 - 6]. Porous medium is a material which is composed of network of pores which has the important properties such as permeability, porosity and tortuosity and are mostly noticed in the fluid flow problems [7, 8]. The numerous applications of porous medium in diversified areas of science, engineering and technology warrant the deeper understanding on the influence of related parameters on the important rheological quantities [9 - 13].

Fluid which has linear relation between its stress and rate of strain is classified as Newtonian fluid; otherwise, it is called as non-Newtonian fluids [14, 15]. This linear association between rate of shear and shear stress in Newtonian fluids is due to the invariable nature of its viscosity coefficient [16]. Air, water, thin motor oil, glycerol, alcohol are some of the familiar examples of Newtonian fluids [17]. In non-Newtonian fluids, the fluid viscosity may vary with respect to either time or spatial variable [18]. Fluids/semi-solids that we use in our day to day life, for example gels, syrups, tooth paste, whipped cream, edible oils, emulsions, varnish, edible oils etc. can be classified into one of the two groups such as Newtonian fluid and non-Newtonian fluid [19 - 21]. The salient physical and rheological characteristics of non-Newtonian fluids motivated several scientists and technologist to explore more of their industrial applications [22, 23]. Among the various non-Newtonian fluids, some fluids exhibit the character of yield stress (i.e. below some threshold level of shear stress, the fluid moves like a solid (is termed as plug flow) and at the stress



level above this threshold limit, the fluid undergoes the usual shear flow [24, 25]. Though, numerous non-Newtonian fluid models exists, only certain fluids can explain the complex behavior of several kinds of natural and industrial flow problems involving porous medium. Casson fluid, Bingham fluid, Herschel-Bulkley (H-B) fluid are yield stress non-Newtonian fluids which have been widely applied in the investigation the various kinds of fluid rheology through porous medium [21 - 23]. The constitutive equations of the aforesaid fluid models are stated hereunder:

$$\text{Casson fluid: } \sqrt{-\mu_c \frac{du}{dy}} = \begin{cases} \sqrt{\tau} - \sqrt{\tau_y} & \text{if } \tau > \tau_y \\ 0 & \text{if } \tau \leq \tau_y \end{cases}, \quad (1a)$$

$$\text{Bingham fluid: } -\mu_b \frac{du}{dy} = \begin{cases} \tau - \tau_y & \text{if } \tau > \tau_y \\ 0 & \text{if } \tau \leq \tau_y \end{cases}, \quad (1b)$$

$$\text{Herschel-Bulkley fluid: } -\mu_h \frac{du}{dy} = \begin{cases} (\tau - \tau_y)^n & \text{if } \tau > \tau_y \\ 0 & \text{if } \tau \leq \tau_y \end{cases}, \quad (1c)$$

where μ_h, μ_c, μ_b , are coefficient of viscosity of H-B fluid, Casson fluid and Bingham fluid respectively; τ_y, τ are the yield stress (threshold limit) and shear stress of the respective fluid; n is the power law index. Casson and Bingham fluid models constitutive equations can be deduced to the constitutive equation of Newtonian fluid when $\tau_y = 0$ [24, 25]. The constitutive equation of H-B fluid model can be deduced to that of Bingham fluid when $n = 1$, power law fluid model when $\tau_y = 0$ is zero and Newtonian fluid model when $n = 1$ and $\tau_y = 0$ [26, 27]. Herschel-Bulkley fluid describes the behavior of shear thinning fluid when $n < 1$ and shear thickening fluid when $n > 1$. Since the constitutive equation of H-B fluid has one more flow parameter, viz. power law index than the other two fluid models, one may obtain more detail on the fluid's rheological characteristics [28]. Moreover, the residual variation between the experimentally observed values and theoretically estimated values of H-B fluid model is substantially less than that of Casson fluid model [29, 30]. Hence, in view of the aforesaid statements, it is highly suitable to model the non-Newtonian fluids flowing under different rheological states as H-B fluid.

The non-Newtonian fluids' flow in porous medium have several applications in diversified fields such as injection of slurries, muds or cement grouts for improving soil strength, glue permeation in the porous medium of solid materials, injecting drilling fluids in rocks for enhancing oil recovery and oil well strengthening, propagation of blood through kidney, blood flow in arterioles and tissues, the flow of viscoplastic fluids in argillaceous soils, pollutants removal from the effluent water treatment plant etc. [31, 32]. Darcy's [33] germinal contribution to the fluid flow in porous media motivated many researchers to investigate further on this kind of flows under different flow geometries and physical considerations [34, 35]. Although naturally there exists different shapes of pores in the porous network of flow medium, the rectangular and circular shapes of pores in the flow medium are encountered more frequently in the engineering applications, such as to enhance heat transfer (through the use of partially filled fibrous porous medium), store heat energy in thermal power stations, store crude oils in reservoirs etc. [36, 37]. Thus, the rectangular and circular geometries of pores network in the flow medium are practically important pore shapes.

Chen et al. [3] analyzed the rheology of Bingham fluid in a porous medium and obtained the macroscopic connection among the flow rate and pressure gradient as function of porous network structure and their research findings have numerous industrial applications including the oil retrieval from oil wells. Balhoff et al. [23] developed effective numerical algorithms for the network modelling of non-Newtonian fluids (without/with yield stress) in porous media and they numerically obtained the threshold gradient. Chevalier et al. [8] analyzed the controlled yield stress fluids' flow in porous media and measured the pressure drop for a wide range of velocities and through detailed data analysis they analytically obtained the expression for pressure drop in terms of flow rate. Oukhlef et al. [38] applied the method of yield stress to find the pattern of pores size distribution in the porous flow medium and this method is successfully verified numerically as well as analytically for the pores size distribution such as multinomial and Gaussian distribution, assuming the fluid as Casson fluid model and Bingham fluid. Experimental studies of Chevalier et al. [39] showed that the yield stress fluid's velocity profile in a connected porous flow medium is almost same as that of Newtonian fluid.

Nash and Rees [40] inspected the effects of microstructure of pores in the uni-directional flow of Bingham fluid in porous flow medium and spelt out that the way by which the fluid pass through at the threshold pressure gradient strongly depends on the distribution of pores sizes. Sankar and Viswanathan [41] mathematically analyzed the steady stream of non-Newtonian Casson fluid in a porous flow medium and reported that Buckingham-Reiner flow rate function is marginally higher in Hagen-Poiseuille (cylindrical pipe) flow than that in plane-Poiseuille flow. The plane-Poiseuille flow and Hagen-Poiseuille flow of H-B fluid in a porous flow medium is not studied by any researcher so far. Hence, the present theoretical study aims to mathematically analyze the effects of porosity, permeability, pressure gradient, period of pipes/channels and radius of pipes/width of channels in the steady laminar flow of H-B fluid in single pipe/single channel and multi-pipes/multi-channels with porous wall and four kinds of probability distributions are used to represent the distribution of pores such as (i) uniform distribution, (ii) Linear distribution of Type I (increasing function), (iii) Linear distribution of type II (decreasing function) and Quadratic distribution. The organization of this research article is briefly described below:

In section 2, the theoretical formulation of fluid flow problem is presented firstly and then the closed form solutions to the flow measurements such as the expressions for fluid's velocity profile, volumetric flow rate, Buckingham-Reiner function, Darcy mean velocity in single pipe/single channel, Darcy mean velocity in multi-pipe/multi-channel, permeability and porosity in Hagen-Poiseuille and plane-Poiseuille flows are obtained. The effects of various flow parameters such as radius of pipe/ width of channel, period of pipes/channels in the porous flow medium, uniform distribution parameter and pressure gradient on the major flow metrics such as Buckingham-Reiner function, Darcy mean velocity, porosity and permeability of the porous flow medium are investigated in Section 3 through the suitable tabular and graphical presentation of data which are computed from the aforesaid flow measurement. Section 4 summarized the main outcomes of this theoretical study. Fig. 1 exhibits the schematic configuration of the fluid flow problem under study.



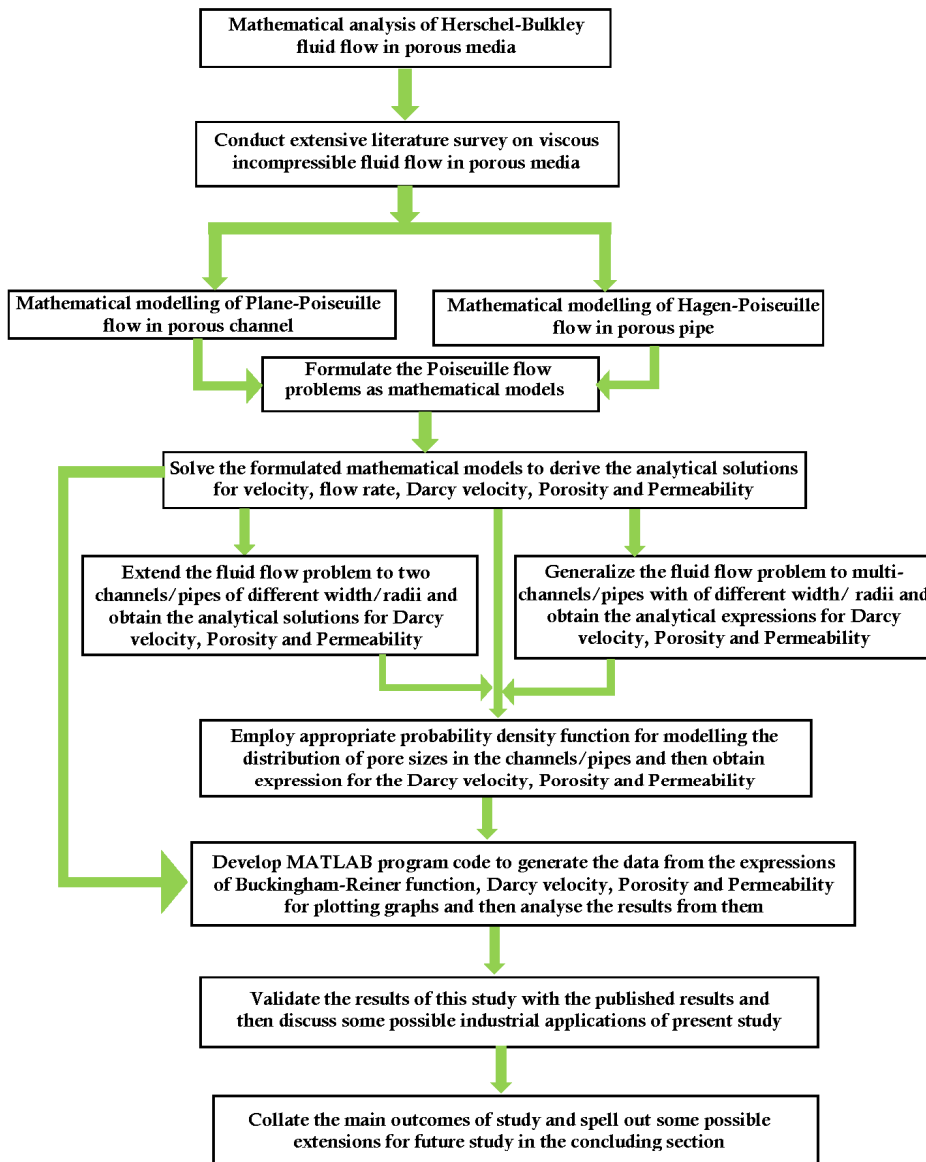
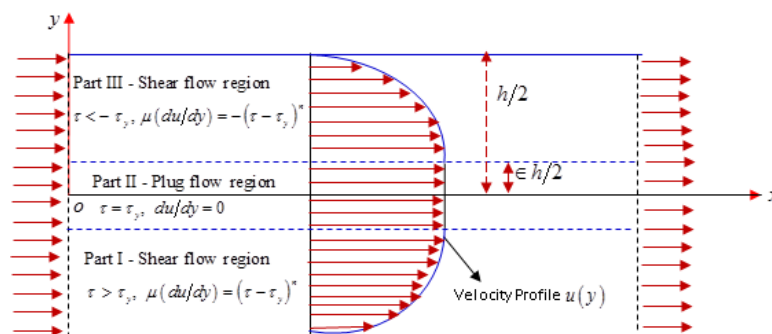


Fig. 1. Schematic plan of the fluid flow system under study.

2. Formulation of mathematical model

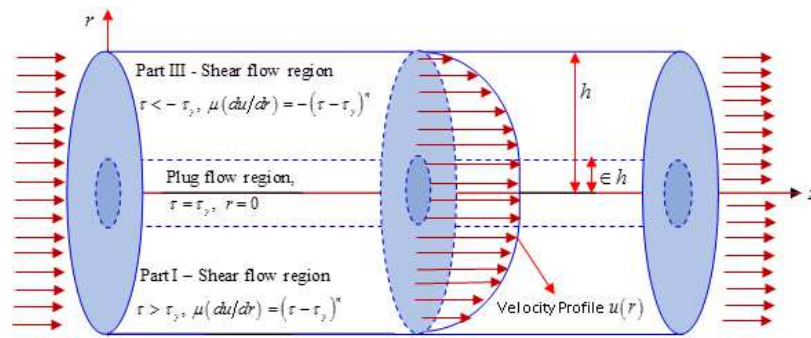
2.1 Plane-Poiseuille flow in a rectangular channel

Consider the uni-directional, fully developed, axi-symmetric and steady plane-Poiseuille flow of viscous incompressible non-Newtonian fluid past a rectangular channel of breadth h which has the boundaries at the planes $y = \pm h/2$. The incompressible non-Newtonian fluid under study is modelled as Herschel-Bulkley (H-B) fluid. The pictorial representations of H-B fluid flow past a rectangular channel and also through a circular pipe are illustrated respectively in Fig. 2(a) and 2(b). The cross-sectional view of the fluid flow past porous media having rectangular pores and circular pores is limned in Figs. 2(c) and 2(d) respectively.

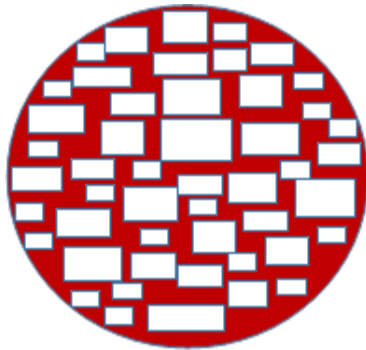


(a) Flow in rectangular channel.

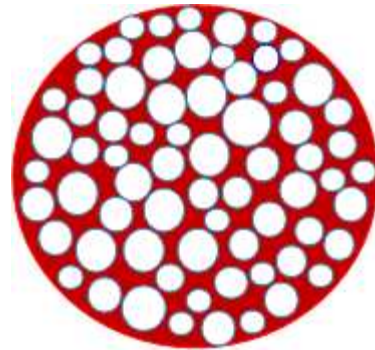




(b) Flow in circular pipe.



(c) Cross sectional geometry of porous medium with rectangular pores.



(d) Cross sectional geometry of porous medium with circular pores.

Fig. 2. Geometries of porous flow medium.

Let $u (= u(y))$ denote the axial velocity of the fluid along the x axis. For the considered uni-directional and isothermal fluid flow, the axial part of the momentum equation reduces to the following form:

$$-\frac{dp}{dx} - \frac{d\tau}{dy} = 0, \tag{2a}$$

where p and $\tau = \tau_{xy}$ are the flowing fluid's pressure and shear stress respectively. The H-B fluid's constitutive equation for its flow in rectangular channel is given as hereunder:

$$\mu \frac{du}{dy} = (\tau - \tau_y)^n \text{ if } \tau > \tau_y, \tag{2b}$$

$$\frac{du}{dy} = 0 \text{ if } -\tau_y < \tau < \tau_y, \tag{2c}$$

$$\mu \frac{du}{dy} = -(\tau - \tau_y)^n \text{ if } \tau < -\tau_y, \tag{2d}$$

where μ is the H-B fluid's viscosity coefficient. The flow conditions at the boundary are expressed as below:

$$u = 0 \text{ at } r = \pm h/2; \quad \tau = 0 \text{ at } y = 0. \tag{3a, 3b}$$

Under the assumed rheological conditions, it is clear that the pressure gradient is always a negative quantity. Let us denote the fluid's pressure gradient $-dp/dx$ by the symbol Ω . Solving Eq. (2a) for shear stress τ and then making use of boundary condition (3b), one can get solution for the shear stress as $\tau = \Omega y$. Since the H-B fluid has non-zero threshold (yield stress), the rheological field in the rectangular channel is split into the following three regions:

$$\text{Region - I: } -\frac{h}{2} \leq y \leq -\frac{\epsilon h}{2} \text{ (Lower Shear flow region),} \tag{4a}$$

$$\text{Region - II: } -\frac{\epsilon h}{2} \leq y \leq \frac{\epsilon h}{2} \text{ (Middle part - Plug flow region),} \tag{4b}$$

$$\text{Region - III: } \frac{\epsilon h}{2} \leq y \leq \frac{h}{2} \text{ (Upper Shear flow region).} \tag{4c}$$



As the flow under study is axi-symmetric, the velocity of the fluid in the upper and lower shear flow regions are identical and hence, it is very adequate to find the expression for velocity in the and in the upper plug-flow region $0 \leq y \leq h/2$ and shear flow regions $h/2 \leq y \leq h/2$. Solving Eqs. (2d) and (3a), we get the expression for H-B fluid's velocity in the upper flow domain and in the plug flow domain as below:

$$u(y) = \frac{\Omega^n}{(n+1)\mu} \left(\frac{h}{2}\right)^{n+1} \left[\left(1 - \frac{y}{(h/2)}\right)^{n+1} - (n+1) \left(1 - \frac{y}{(h/2)}\right)^n + \frac{n(n+1)\epsilon^2}{2} \left(1 - \frac{y}{(h/2)}\right)^{n-1} \right] \text{ if } \frac{\epsilon h}{2} \leq y \leq \frac{h}{2}, \tag{5a}$$

$$u_p = \frac{\Omega^n}{(n+1)\mu} \left(\frac{h}{2}\right)^{n+1} \left[1 - (n+1)\epsilon + \frac{n(n+1)\epsilon^2}{2} - \frac{n(n-1)\epsilon^{n+1}}{2} \right] \text{ if } -\frac{\epsilon h}{2} \leq y \leq \frac{\epsilon h}{2}, \tag{5b}$$

where $\epsilon = 2\tau_y / \Omega h$ is the dimensionless form of threshold which denotes the proportion of the flow region where the plug flow occurs. The velocity profile given by Eq. (5a) is effective only if $\epsilon < 1$. When $\epsilon > 1$, then the plug flow happens in the entire flow region of the channel. Let $\sigma = 1/\epsilon$, then σ is the dimensionless form of pressure gradient which mainly depends on the fluid's yield stress. One can note that the fluid starts to flow when σ raises above unity and hence $\sigma = 1$ is the pressure gradient's threshold level. Assuming the flow field as Purcell's [42] type of porous medium, the shape of the pores in the porous medium are generally considered as either rectangular (channels) with different widths or circular (pipes) with different radii. Thus, adopting Purcell [42] type of porous flow medium to the present fluid flow study, the shape of the pores in the flow field of plane-Poiseuille flow and Hagen-Poiseuille flow are considered as rectangular channel of different width and circular tube of different radii respectively. As the first case, we assume that one period H of pores in flow field of plane-Poiseuille flow consist of one rectangular pore (channel) of width h and an another rectangular pore (channel) of width γh , where $\gamma < 1$.

The expression for total flow rate Q for flow in one channel of width h is obtained as hereunder:

$$Q = \int_{-h/2}^{h/2} u(y) dy = 2 \left[\int_0^{\epsilon h/2} u_p dy + \int_{\epsilon h/2}^{h/2} u(y) dy \right] = \frac{2\Omega^n}{(n+2)\mu} \left(\frac{h}{2}\right)^{n+2} f(\sigma) = \frac{2\tau_0}{(n+2)\mu} \left(\frac{h}{2}\right)^{n+1} \sigma^n f(\sigma), \tag{6a}$$

where

$$f(\sigma) = \begin{cases} 1 - \frac{n(n+2)}{(n+1)|\sigma|} + \frac{(n-1)(n+2)}{2|\sigma|^2} - \frac{n(n^2-3)}{2(n+1)|\sigma|^{n+2}} & \text{if } |\sigma| > 1 \\ 0 & \text{otherwise} \end{cases} \tag{6b}$$

The expression obtained for $f(\sigma)$ in Eq. (6b) may be called as the Buckingham - Reiner function for the plane - Poiseuille flow of H-B fluid. One can observe that when $\tau_y = 0$ (i.e. $\epsilon = 1/\sigma \neq 0$) and $n = 1$, H-B fluid's constitutive equation deduces to Bingham fluid's constitutive equation and in this case, the expressions derived for the flow rate in Eq. (6a) and (6b) for plane-Poiseuille flow and in Eq. (A1) (refer the Appendix) for Hagen-Poiseuille flow are in exact agreement with the expressions obtained by Nash and Rees [40] in their Eqs. (6) and (48) respectively. Since, we confine the negative of the pressure gradient Ω as positive flow quantity, σ tends to be a positive quantity and thus hereafter we use σ in place of $|\sigma|$. The Darcy velocity of H-B fluid u_H is its mean velocity which is obtained over one period of distribution of channels as given below:

$$u_H = \frac{\varphi \Omega^n}{(n+2)\mu} \left(\frac{h}{2}\right)^{n+1} f(\sigma) = \frac{\Omega^n K}{\mu} f(\sigma), \tag{7}$$

where

$$K = \frac{\varphi}{(n+2)} \left(\frac{h}{2}\right)^{n+1} \text{ and } \varphi = \frac{h}{H}, \tag{8a,b}$$

are the expressions for porosity and permeability of porous flow medium respectively and H is the period of distribution of channels. These are some of the major rheological parameters of the present study which mainly depends on the channels' choice and are applied in computing the period of porous medium. The vital criteria for the occurrence of the normal flow is that $\sigma \gg 1$. From Eq. (7), we get the mean velocity of Newtonian fluid flow as $u_N = \Omega K / \mu$. The normalized form of mean velocity $f(\sigma)$ of H-B fluid (ratio between the mean velocities of H-B and Newtonian fluids for flow in channel) in plane-Poiseuille flow is defined as below:

$$f(\sigma) = u_H / u_N \tag{9}$$

From Eq. (6b), it is observed that $f(\sigma) \rightarrow 1$ as $\sigma \rightarrow \infty$. The normalized mean velocity $f(\sigma)$ near the threshold values deduce to the quadratic form as below:

$$f(\sigma) = \frac{1}{2}(n-1)(n-2)(n+2)(\sigma-1) - \frac{1}{4}(n-2)(n+2)(n^2+4n-3)(\sigma-1)^2 + \frac{1}{12}(n+2)(n^4+6n^3+3n^2-48n+24)\dots, \quad 0 < (\sigma-1) < < 1 \tag{10}$$

For quite large values of σ , H-B fluid model shows the characteristics of Newtonian fluid. For large values of σ , the two-term approximation to the induced flow $\sigma f(\sigma)$ can be derived as



$$\sigma f(\sigma) \approx \sigma - \frac{n(n+2)}{(n+1)}, \quad \text{if } \sigma \gg 1 \quad (11)$$

From Eq. (11), one can define the pseudo-threshold value of pressure gradient σ as

$$\sigma_{pt} = \frac{n(n+2)}{(n+1)} \quad (12)$$

Corresponding to the flow quantities obtained in Eqs. (6) – (11) for plane-Poiseuille flow, the similar flow quantities for the Hagen-Poiseuille flow (flow in circular pipe) are obtained in Appendix, where $g(\sigma)$ is the normalized mean velocity in the circular tube of radius h . Hereafter, we use the notations $F(\sigma)(=u_c/u_N)$ and $G(\sigma)(=u_c/u_N)$ to denote the normalized velocities of H-B fluid flow in rectangular channel and circular tube respectively.

2.2 Effect of two channels of different width

Although some particular kinds of fluid flow applications (e.g. chemical processes, medical treatments, biological experiments etc.) encounters different shapes of pores in their flow medium viz., elliptical, square, triangular, pentagonal, hexagonal etc., the rectangular and circular shapes of pores in the flow medium are used in some specific kinds of fluid flow applications, viz., physiological flows such as blood flow in arterioles, capillaries, tissues, blood flow in devices used for clinical bio-chemistry etc., and engineering applications such as flow in petroleum reservoirs, magnetohydrodynamic generators, etc. [43, 44]. Thus, the present study considers the shape of pores in flow medium as rectangular (for plane-Poiseuille flow) and circular (for Hagen-Poiseuille flow). Let us first consider the porous medium with one period of channels which comprised of two channels, of which the first (wide) channel has width h and second (narrow) channel has width γh , where $\gamma < 1$. The total flow rate of H-B fluid flow in one period of channels is defined by the following formula [40]:

$$Q = \frac{2\Omega^n}{(n+2)\mu} \left(\frac{h}{2}\right)^{n+2} [f(\sigma) + \gamma^{n+2}f(\gamma\sigma)]. \quad (13)$$

The Darcy velocity of H-B fluid flow is

$$u_H = \left(\frac{\Omega^n K}{\mu}\right) [f(\sigma) + \gamma^{n+2}f(\gamma\sigma)] / (1 + \gamma^{n+2}). \quad (14)$$

The mean velocity of H-B fluid flow relative to the flow rate of Newtonian fluid flow is

$$u_H/u_N = F(\sigma) = [f(\sigma) + \gamma^{n+2}f(\gamma\sigma)] / (1 + \gamma^{n+2}). \quad (15)$$

The expressions for permeability and porosity in the channel porous medium are obtained respectively as

$$K = \frac{\varphi(1 + \gamma^{n+2})}{(n+2)(1 + \gamma)} \left(\frac{h}{2}\right)^{n+1}; \quad \varphi = (1 + \gamma)h/H, \quad (16a,b)$$

For large values of σ ($\sigma \gg 1$), the two-term approximation to the mean velocity is obtained as

$$\sigma F(\sigma) \approx \sigma - \frac{n(n+2)(1 + \gamma^{n+1})}{(n+1)(1 + \gamma^{n+2})}. \quad (17)$$

From Eq. (17), one can deduce the pseudo-threshold value of the pressure gradient σ as

$$\sigma_{pt} = \frac{n(n+2)(1 + \gamma^{n+1})}{(n+1)(1 + \gamma^{n+2})}. \quad (18)$$

2.3 Effect of multi-channels of different widths

We can extend the two-channels in one period of porous flow medium to a general case of N channels per period of porous flow medium. Let the width of the channels N be $\gamma_i h$ for $i=1,2,\dots,N$ and suppose the channels in the porous medium are arranged in the descending order of their width, then one can have the following inequality:

$$1 = \gamma_1 \geq \gamma_2 \geq \dots \gamma_N. \quad (19)$$

The Darcy velocity of H-B fluid flow through porous medium having N channels per period is defined as

$$u_H = \left(\frac{\Omega^n K}{\mu}\right) \left[\frac{\sum_{i=1}^N \gamma_i^{n+2} f(\gamma_i \sigma)}{\sum_{i=1}^N \gamma_i^{n+2}} \right]. \quad (20)$$

The expressions for permeability and porosity of the porous flow medium with N channels per period are defined as below:

$$K = \left(\frac{\varphi}{n+2}\right) \left(\frac{h}{2}\right)^{n+1} \left[\frac{\sum_{i=1}^N \gamma_i^{n+2}}{\sum_{i=1}^N \gamma_i} \right]; \quad \varphi = \left(\frac{h}{H}\right) \sum_{i=1}^N \gamma_i. \quad (21a,b)$$

The normalized mean velocity of H-B fluid relative to that of Newtonian fluid is defined by



$$u_H/u_N = F(\sigma) = \left[\frac{\sum_{i=1}^N \gamma_i^{n+2} f(\gamma_i \sigma)}{\sum_{i=1}^N \gamma_i^{n+2}} \right] \tag{22}$$

For Hagen-Poiseuille flow of H-B fluid in a porous flow medium which is framed of multi-circular tubes, the expressions similar to (20) – (22) are obtained in Appendix A3.

2.4 Probability density functions for pores

The pores in the porous medium are often dispersed in some particular pattern which can be represented by some appropriate probability distributions. In this study, to analyze the influence of porosity as well as permeability of porous flow medium on the rheological quantities, the dispersion of the width of channels in the porous medium is represented by distinct continuous probability distributions such as (i) Uniform distribution, (ii) Linear distributions (of two types) and (iii) Quadratic distribution. Let us denote the probability density function of the channels’ widths in the porous flow medium by $\psi(\gamma)$. Using Eqs. (20) – (22), the expression for normalized Darcy (mean) velocity of H-B fluid flow in a porous flow medium with multi-channels relative to that of the Newtonian fluid flow, the porosity and permeability of the porous flow medium can be computed as below [40].

$$F(\sigma) = \int_0^\infty \gamma^{n+2} \psi(\gamma) f(\gamma \sigma) d\gamma / \int_0^\infty \gamma^{n+2} \psi(\gamma) d\gamma, \tag{23a,b}$$

$$K = \left[\frac{\varphi}{(n+2)} \left(\frac{h}{2} \right)^{n+1} \right] \frac{\int_0^\infty \gamma^{n+2} \psi(\gamma) d\gamma}{\int_0^\infty \gamma \psi(\gamma) d\gamma}; \quad \varphi = \left(\frac{h}{H} \right) \int_0^\infty \gamma \psi(\gamma) d\gamma. \tag{24}$$

2.4.1 Uniform distribution

Let the pores of the flow medium be uniformly distributed, then its probability density function is given by

$$\psi(\gamma) = \begin{cases} \frac{1}{1-a} & \text{if } a < \gamma < 1 \\ 0 & \text{otherwise} \end{cases} \tag{27}$$

The normalized Darcy velocity of H-B fluid in a porous medium with multi-channels with uniformly distributed pores is

$$F(\sigma) = \begin{cases} 0 & \text{if } 0 \leq \sigma < 1 \\ \frac{\left[2(n+1)\sigma^{n+3} - 2n(n+3)\sigma^{n+2} + (n-1)(n+2)(n+3)\sigma^{n+1} \right] - n(n^2-3)(n+3)\sigma + (n^4+2n^3-5n^2-6n+4)}{2(n+1)(1-a^{n+3})\sigma^{n+3}} & \text{if } 1 \leq \sigma \leq 1/a \\ \left[1 - \frac{n(n+3)(1+a+a^2+\dots+a^{n+1})}{(n+1)(1+a+a^2+\dots+a^{n+2})\sigma} + \frac{(n-1)(n+2)(n+3)(1+a+a^2+\dots+a^n)}{2(n+1)(1+a+a^2+\dots+a^{n+2})\sigma^2} \right] - \frac{n(n^2-3)(n+3)}{2(n+1)(1+a+a^2+\dots+a^{n+1})\sigma^{n+2}} & \text{if } \sigma > \frac{1}{a} \end{cases} \tag{28}$$

From Eq. (28), one can observe that depending on the range of the values of dimensionless pressure gradient σ (given in Eq. (28)), the whole flow region is split into three parts. In part I ($0 \leq \sigma < 1$), no flow occurs (flow is stagnant), whereas in part II of the flow region ($1 \leq \sigma \leq 1/a$), the flow happens in the part of the channels whose width ranges from h/σ to h . In the third part of the flow regime ($\sigma > 1/a$), the fluid flow occurs in all the channels. For this kind of flow (in channels with uniformly distributed pores), the permeability and porosity are obtained as

$$K = \frac{2\varphi(1-a^{n+3})}{(n+2)(n+3)(1-a^2)} \left(\frac{h}{2} \right)^{n+1}; \tag{29}$$

$$\varphi = \left(\frac{h}{H} \right) \left(\frac{1+a}{2} \right). \tag{30}$$

When $a = 0$ (when the channels width don’t have a lower limit), then the third part of the flow region no longer exists and thus, one can get the simplified expression for normalized Darcy velocity as given below:



$$F(\sigma) = \begin{cases} 0 & \text{if } 0 \leq \sigma < 1 \\ \frac{2(n+1)\sigma^{n+3} - 2n(n+3)\sigma^{n+2} + (n-1)(n+2)(n+3)\sigma^{n+1} - n(n^2-3)(n+3)\sigma + (n^4+2n^3-5n^2-6n+4)}{2(n+1)\sigma^{n+3}} & \text{if } 1 \leq \sigma \leq 1/a \end{cases} \quad (31)$$

When the dimensionless pressure gradient σ is quite large ($\sigma \gg 1$), from Eq. (31) we obtain the pseudo-threshold of pressure gradient as

$$\sigma_{pt} = \frac{n(n+3)(1+a+a^2+\dots+a^{n+1})}{(n+1)(1+a+a^2+\dots+a^{n+2})}. \quad (32)$$

2.4.2 Linear distribution

The density functions of two linear probability distributions which are used to model the dispersion width of the pores in the porous medium are defined hereunder:

$$(i) \quad \psi(\gamma) = 2\gamma, \quad 0 \leq \gamma \leq 1; \quad (33)$$

$$(ii) \quad \psi(\gamma) = 2(1-\gamma), \quad 0 \leq \gamma \leq 1. \quad (34)$$

It is noted that the first linear distribution (defined in Eq. (33)) is a function that increases monotonically, meaning that the channels width increases as γ raises; whereas the second linear distribution is a monotonically decreasing function, which implies that the channel width decreases with the rise of the channel width ratio parameter. For first linear distribution (defined in Eq. (33)), the expressions for normalized Darcy velocity, permeability and porosity are derived as Eqs. (35) – (37).

$$F(\sigma) = \begin{cases} 0 & \text{if } 0 \leq \sigma \leq 1 \\ \frac{4(n+1)(n+3)\sigma^{n+4} - 4n(n+2)(n+4)\sigma^{n+3} + 2(n^2-1)(n+3)(n+4)\sigma^{n+2} - (n^2-3)n(n+3)(n+4)\sigma^2 + (n^5+5n^4-n^3-23n^2-6n+12)}{4(n+1)(n+3)\sigma^{n+4}} & \text{if } \sigma > 1 \end{cases} \quad (35)$$

$$SK = \frac{3\varphi}{(n+2)(n+4)} \left(\frac{h}{2}\right)^{n+1}; \quad \varphi = \frac{2}{3} \left(\frac{h}{H}\right). \quad (36a,b)$$

For quite large values of σ ($\sigma \gg 1$), one can deduce the pseudo-pressure gradient from Eq. (35) as below in Eq. (37):

$$\sigma_{pt} = \frac{n(n+2)(n+4)}{(n+1)(n+3)}. \quad (37)$$

For the second type of linear distribution (given in Eq. (34)), the analytical expressions of normalized mean velocity, permeability and porosity are obtained as in Eqs. (38) – (39).

$$F(\sigma) = \begin{cases} 0 & \text{if } 0 \leq \sigma \leq 1 \\ \frac{4(n+1)\sigma^{n+4} - 4n(n+4)\sigma^{n+3} + 2(n-1)(n+3)(n+4)\sigma^{n+2} - n(n+3)(n+4)(n^2-3)\sigma^2 + 2(n+4)(n^4+2n^3-5n^2-6n+4)\sigma - (n^5+5n^4-n^3-23n^2-6n+12)}{4(n+1)\sigma^{n+4}} & \text{if } \sigma > 1 \end{cases} \quad (38)$$

$$K = \frac{6\varphi}{(n+2)(n+3)(n+4)} \left(\frac{h}{2}\right)^{n+1}; \quad \varphi = \frac{1}{3} \left(\frac{h}{H}\right) \quad (39a,b)$$

When the pressure gradient takes larger values σ ($\sigma \gg 1$), from Eq. (38), one can deduce the pseudo threshold value of the pressure gradient as Eq. (40):

$$\sigma_{pt} = \frac{n(n+4)}{(n+1)}. \quad (40)$$

2.4.3 Quadratic distribution

The density functions of quadratic probability distributions is given below:

$$\psi(\gamma) = 3(1-\gamma)^2, \quad 0 \leq \gamma \leq 1; \quad (41)$$

By applying the quadratic distribution to model the width of the pores in the porous flow medium which is composed of multi-channels, one can derive the expressions for normalized Darcy velocity, porosity and permeability simplifies to Eqs. (42) – (43a; 43b), respectively.



$$F(\sigma) = \begin{cases} 0 & \text{if } 0 \leq \sigma \leq 1 \\ \left. \begin{aligned} &12(n+1)\sigma^{n+5} - 12n(n+5)\sigma^{n+4} + 6(n-1)(n+4)(n+5)\sigma^{n+3} \\ &-n(n^2-3)(n+3)(n+4)(n+5)\sigma^3 + 3(n+4)(n+5)(n^4+2n^3-5n^2-6n+4)\sigma^2 \\ &-3(n+5)(n^5+5n^4-n^3-23n^2-6n+12)\sigma + (n+1)(n+2)(n^4+6n^3-3n^2-36n+24) \end{aligned} \right\} & \text{if } \sigma > 1 \end{cases} \quad (42)$$

$$K = \frac{24\varphi}{(n+2)(n+3)(n+4)(n+5)} \left(\frac{h}{2}\right)^{n+1}; \quad \varphi = \frac{1}{4} \left(\frac{h}{H}\right). \quad (43a,b)$$

For considerably large values of σ ($\sigma \gg 1$), the pseudo-threshold pressure gradient can be deduced from Eq. (42) as given below:

$$\sigma_{pt} = \frac{n(n+5)}{(n+1)}. \quad (44)$$

Since H-B fluid's constitutive equation deduces to that of Bingham fluid model when the power law index $n = 1$ and in such a case, the expressions obtained so far to various rheological measures (such as velocity, Buckingham-Reinner function, Darcy velocity, permeability, porosity etc.) reduce to that respective flow quantities of Bingham fluid model and the reduced analytical solutions for the rheological quantities are in exact agreement with the respective analytical solutions obtained by Nash and Rees [40] for Bingham fluid and this comparison validates the present study.

2.4.4 Vindication for choosing special probability density functions

In various real word and industrial engineering applications, the fluid flow occurs through porous medium that has rectangular (channels)/circular (pipes) shapes of pores and the distribution of widths of rectangular channels/radii of circular pipes follow either some particular pattern of random structure [6, 38]. Oukhelf [38] propounded that the size of pores in the porous flow medium/porous network (composed of pipes/channels) can be determined from the analytical/numerical solution of integral equation which is formulated from the principles of total flux in fluid flow and the fluid's constitutive equation. Through the theoretical investigation, Oukhelf [38] confirmed that the pores size distribution of pipes/channels in the porous flow medium obtained through the analytical/numerical solution are in good agreement with the respective values computed from the probability density function (PDF) of normal distribution (refer Fig. 5 in Ref. [38]). Oukhelf [38] also reported that the computing of pore sizes distribution from the PDF is much easier than computing the respective values by solving the Volterra integral equation analytically or numerically. Thus, on considering the computational efficiency of pores (width of channels/radii of pipes) size distribution in porous medium/network, we use three different kinds of PDFs such as (i) uniform distribution, (ii) two types of linear distributions and (iii) quadratic distributions. It is believed that these three kinds of PDFs would cover the wide range of pores sizes and patterns (channels width/pipes radius) in the porous flow medium which we come across in various fluid flow applications involving porous media such as filtering toxic wastages in effluent treatments plants, absorbing salts in mineral water purification processes, absorbing toxic bio-fluids in biological tissues, diffusing of drugs in the circulatory systems of human body, water absorbance by several kinds of river beds etc.

3. Numerical simulation of results and discussion

The primary aim of this mathematical analysis is to examine the influence of rheological parameters viz, the radius h of circular pipe/width h of rectangular channel, negative of pressure gradient σ of the fluid flow, period σ of circular pipes/rectangular channels distribution in the porous flow medium on the crucial flow characteristics such as Buckingham-Reiner function $f(\sigma)$ (or $g(\sigma)$), Darcy mean velocity u_c/u_N , permeability K and porosity φ and of the porous flow medium, in the one-directional flow of H-B fluid in a rectangular channel (plane-Poiseuille flow) /circular pipe (Hagen-Poiseuille flow) which has the features of permeability and porosity. The different parameters and the justification for the choice of their range of values used in this theoretical study are briefed below [29, 40, 41]:

The values of pressure gradient parameter σ are chosen in the range 1–5, since no shear flow occurs if $\sigma < 1$ (i.e. the fluid flow in the whole region becomes unyielded if $\sigma < 1$) and also as slow flow is assumed, the upper limit of the pressure gradient is confined to 6. To cover the broader range of multi-pipes radii/multi-channels width, the ranges of the single-pipe radius/single-channel width parameter h and multi-pipes radii/multi-channels width ratio parameter γ are chosen as 0.7–1.0 and 0.5–1 respectively [40]. To investigate the effects of various types of pipes/channels distribution on the permeability and porosity of porous flow medium, the range of the period of pipes/channels parameter H is chosen as 1–11 [41]. Similarly, to study the changes in the porosity and permeability of porous flow domain for various values of uniformly distributed pipes radii/channels width, its parameter 'a' is chosen in the interval (0,1) as adopted by Nash and Rees [33]. Some industrial and natural applications of these kinds of flow covering the aforesaid range of parameter values are injecting cement in soils, glue penetration in porous medium, polymer processing in injection molding, packed beds etc. [38, 39].

It is to be noted here that in the plots of all the graphs presented in this section, dotted red lines denote the flow characteristics in Hagen-Poiseuille flow, while the continues blue lines refer to the flow quantities' variation in plane-Poiseuille flow.

3.1 Buckingham-Reiner function

The variation of Buckingham-Reiner function $f(\sigma)$ (or $g(\sigma)$) (normalized flow rate) with the rise of pressure gradient σ in the plane-Poiseuille and Hagen-Poiseuille flows of H-B fluid past porous medium is delineated in Fig. 3a. One can notice that in both kinds of flow, Buckingham-Reiner function increases linearly with the raise of pressure gradient from 1 to 2.5 and it increases slowly (nonlinearly) with the rise of pressure gradient σ from 2.5 to 5. In both plane-Poiseuille and Hagen-Poiseuille flows, the Buckingham-Reiner function increases substantially when the parameter n raises. When the values of parameters σ and m are



held constant, the Buckingham-Reiner function is slightly higher in flow through pipe than in flow through channel. Fig. 3b sketches the variation in the dimensionless Buckingham-Reiner function with pressure gradient for various values of the parameter n . One can also observe that the dimensionless Buckingham-Reiner function rises linearly (steadily) when the pressure gradient σ raises from 1 to 5. It is well known that H-B fluid model's constitutive equation reduces to that of Bingham fluid model when the parameter $n = 1$. The plots of the Buckingham-Reiner function and dimensionless Buckingham-Reiner function of Herschel-Bulkley fluid with $n = 1$ (for Bingham fluid) in plane-Poiseuille flow and Hagen-Poiseuille flow depicted in Figs. 3a and 3b respectively are in very good agreement with the corresponding plots of Nash and Rees [40] in their Figs. 1a and 1b for Bingham fluid and this comparison validates the present study.

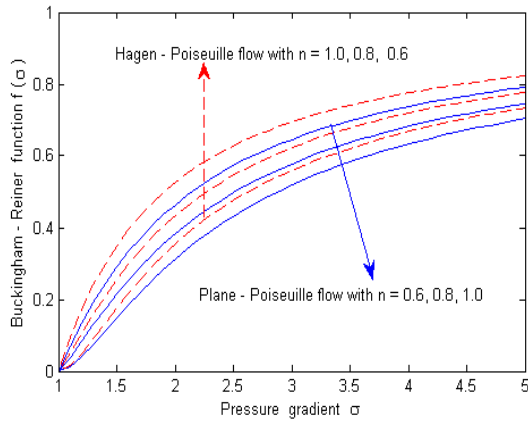


Fig. 3a. Variation in Buckingham – Reiner function $f(\sigma)$ with respect to pressure gradient σ for various values of the parameter n .

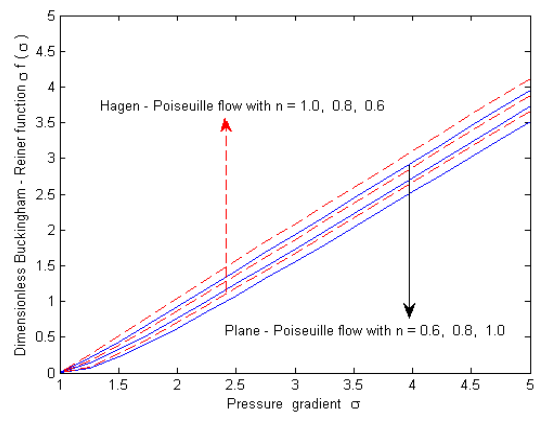


Fig. 3b. Dimensionless Buckingham – Reiner function $\sigma f(\sigma)$ Vs pressure gradient $f(\sigma)$ for different values of the parameter n .

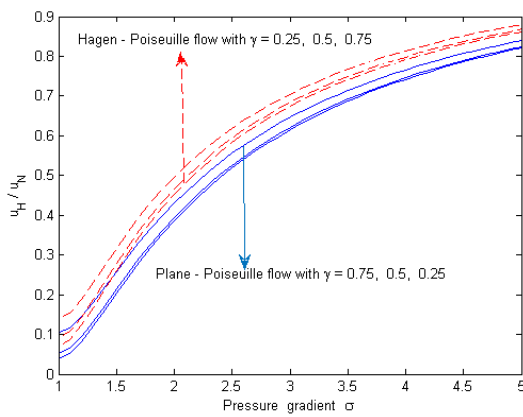


Fig. 4a. Variation of Darcy mean velocity with pressure gradient for various values of channel / pipe widths /radii scaling parameter γ with $n = 1$.

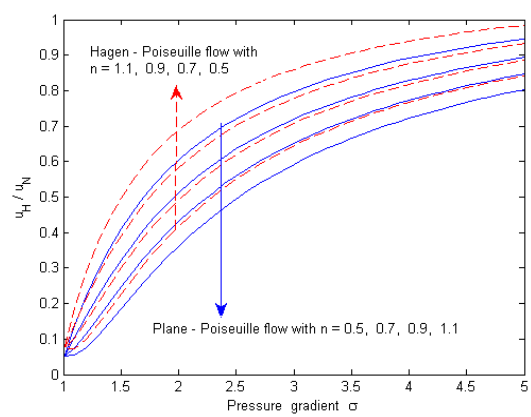


Fig. 4b. Variation of Darcy mean velocity with pressure gradient for distinct values power law index with $\gamma = 0.75$.

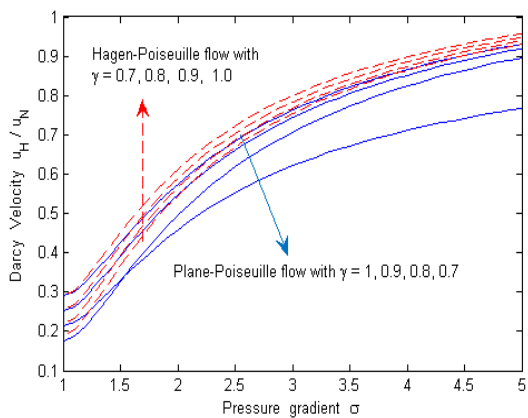


Fig. 5a. Variation of Darcy velocity with pressure gradient in multi-channel/pipes for distinct values of γ with $n = 1.1$.

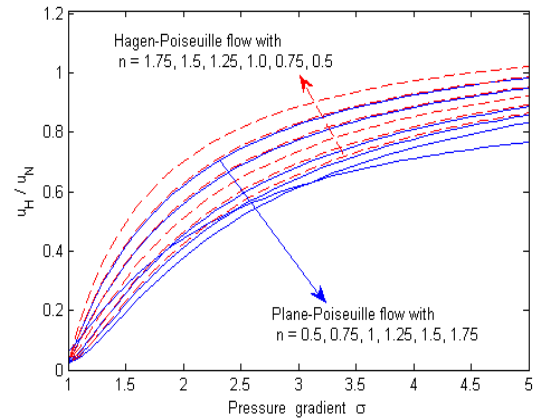


Fig. 5b. Variation of Darcy velocity with pressure gradient in multi-channel/pipes for distinct values of n with $\gamma = 0.8$.



3.2 Darcy Mean velocity in single channel/single pipe and multi-channels/multi-pipes

The effects pressure gradient parameter σ and channels width/pipes radii scaling parameter γ on the Darcy mean velocity u_H/u_N with $n=1$ are depicted in Fig. 4a. One can note that the Darcy velocity soars up with the rise of pressure gradient from 1 to 3 and then it increases slowly when pressure gradient raises further from 3 to 5. When the pressure gradient is kept as constant and the channel width/pipe radii scaling parameter γ increases, the Darcy velocity increases marginally. When all the parameters are treated as invariable, the Darcy mean velocity of fluid is considerably higher for flows in circular pipe than in rectangular channel. Fig. 4b illustrates the variation of Darcy velocity u_H/u_N with pressure gradient σ for distinct values of n with $\gamma=0.75$. One can record that the H-B fluid's Darcy velocity fluid decreases substantially with the rise of power law index parameter n .

3.3 Darcy velocity in multi-channels / multi-pipes

Fig. 5a depicts the variation in Darcy velocity with respect to pressure gradient in the fluid flow through multi-pipes of radii/multi-channels of multi-pipes radii / multi-pipes of widths scaling parameter $\gamma=0.8, 0.9$ and 1 with $n=1.1$. It is noticed that the Darcy velocity increases rapidly when the pressure gradient σ raises from 1 to 2.5 and then it increases slowly with the rise of pressure gradient σ from 2.5 to 5. When the values of pressure gradient and power law index n are kept as constant, the Darcy mean velocity raises substantially with the raise of the width of multi-channels and increases marginally with the rise of the radii of the multi-pipes. It is also seen that the Darcy mean velocity of fluid is substantially higher in Hagen-Poiseuille flow than in plane-Poiseuille flow when all of the other parameters are treated as invariable. The variation of Darcy mean velocity of fluid with pressure gradient σ for distinct values of power law index parameter with $\gamma=0.8$ is exhibited in Fig. 5b. One can point out that the fluid's Darcy mean velocity increase linearly (gradually) with the rise of pressure gradient σ from 1 to 2.5 and then it rises very slowly (almost constant) with the increase of pressure gradient σ from 2.5 to 5. When the pressure gradient σ and the multi-channels width/ multi-pipes radii parameter γ are treated as invariable, the Darcy mean velocity of the fluid reduces marginally when the power law index parameter n raises. From Figs. 5a and 5b, one can notice that in both plane Poiseuille flow and Hagen-Poiseuille flow, the Darcy velocity increases monotonically with the raise of the pressure gradient parameter σ which is generally quite natural. One can also observe that for a given set of values of all the parameters, the Darcy velocity is marginally higher in Hagen-Poiseuille flow than in plane-Poiseuille flow.

3.4 Darcy Mean velocity in channels/pipes with various kinds of pores distribution

The variation in fluid's Darcy mean velocity with pressure gradient for flow in multi- pipes/multi-channels (with uniformly distributed pores) for different values of uniform distribution parameter a when power law index $n=1$ is plotted Fig. 6. When the uniform distribution parameter a is 0.2, 0.4 or 0.6, H-B fluid's Darcy mean velocity rises linearly (gradually) with the rise of pressure gradient from 1 to 3 and it increases very slowly with the further rise of pressure gradient from 3 to 6. But, when the uniform distribution parameter a is 0.8, Darcy mean velocity shoots up sharply when pressure gradient increases from 0 to 3 and then it raises linearly (gradually) with the rise of pressure gradient from 3 to 6. One can also note that the fluid's mean velocity is slightly higher in flow through circular pipe than in flow through rectangular channel.

Fig. 7 exhibits the variation in mean velocity with respect to pressure gradient σ in plane-Poiseuille flow for distinct values of power law index parameter n when the pores follow four kinds of probability density functions (a. Uniform distribution with $a=0.5$; b. Linear distribution of Type-I; c. Linear distribution of Type-II and d. Quadratic distribution). One can also note that in the uniform and linear types (I and II) of pores distribution, the Darcy mean velocity, soars up when the pressure gradient rises from 1 to 3.5 and then it ascends gradually (linearly) when the pressure gradient raises further from 3.5 to 6. Whereas, when the pores in the flow medium are quadratically distributed, the Darcy mean velocity raises linearly when the pressure gradient raises from 1 to 6. It is also recorded that when all the parameters values are held as constant, the Darcy mean velocity is higher (by 6.25%) when the pores width in the flow medium are uniformly distributed than when the pores are dispersed in linear distribution of type I. The mean velocity is higher (by 10%) when the pores are scattered in linear distribution of type I than when the pores in the flow medium follow linear distribution of type II. It is further noted that the mean velocity is higher (by 11.5%) when the pores are distributed in linear distribution of type II than when the pores of the flow medium follow quadratic distribution. It is also pronounced that the H-B fluid's mean velocity fluid descends marginally when the power law index parameter n increases.

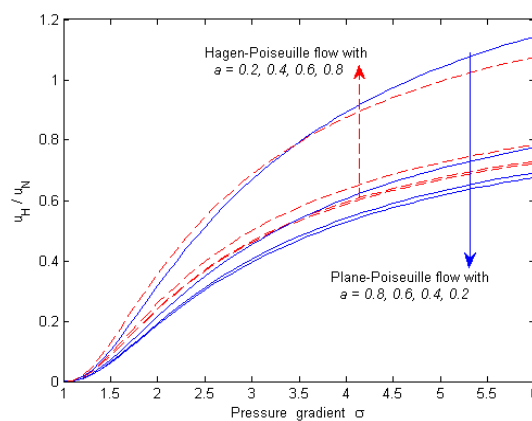


Fig. 6. Variation of Darcy mean velocity with pressure gradient in multi-channel/pipes for various values of uniform distribution parameter a with $n=1$.



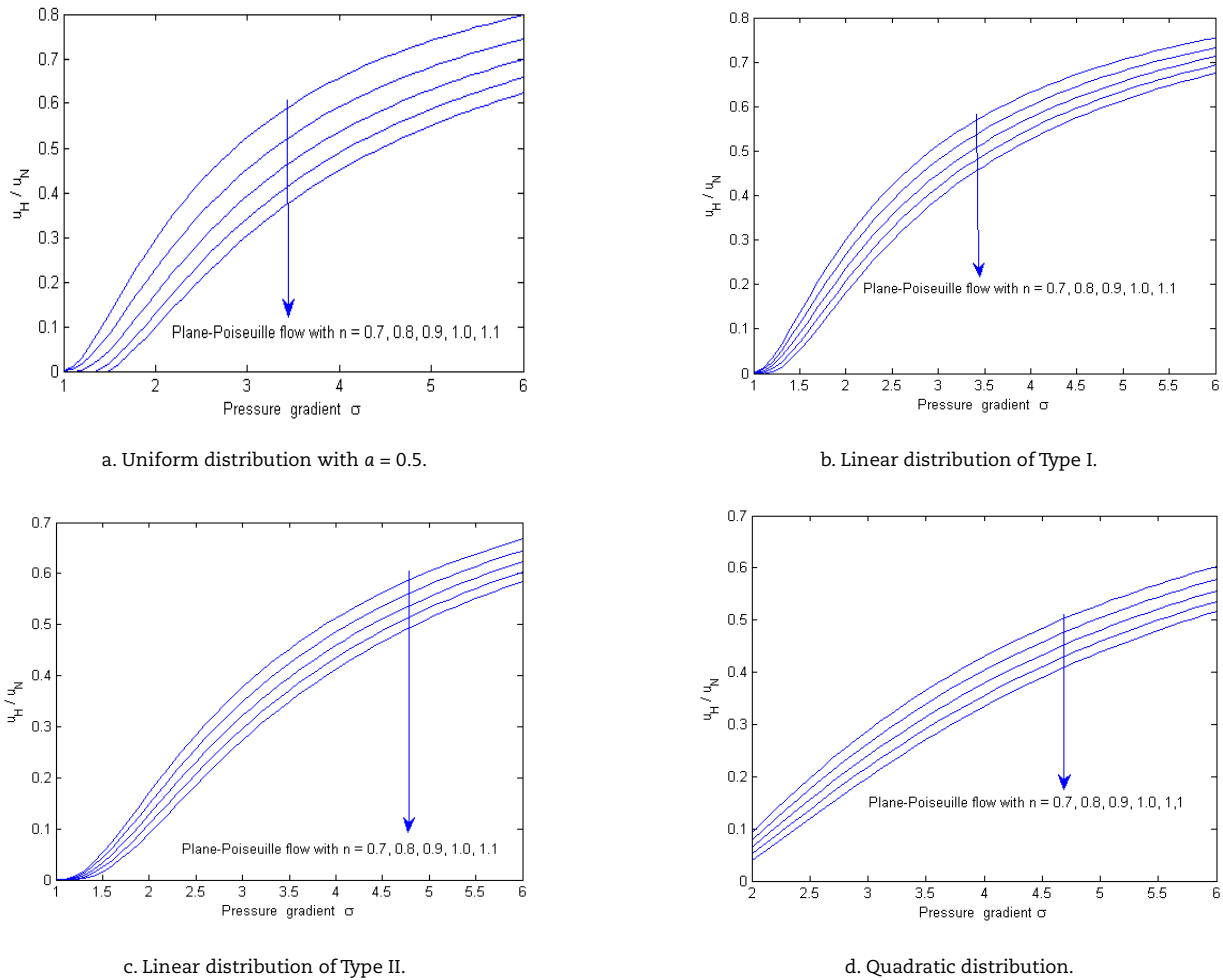
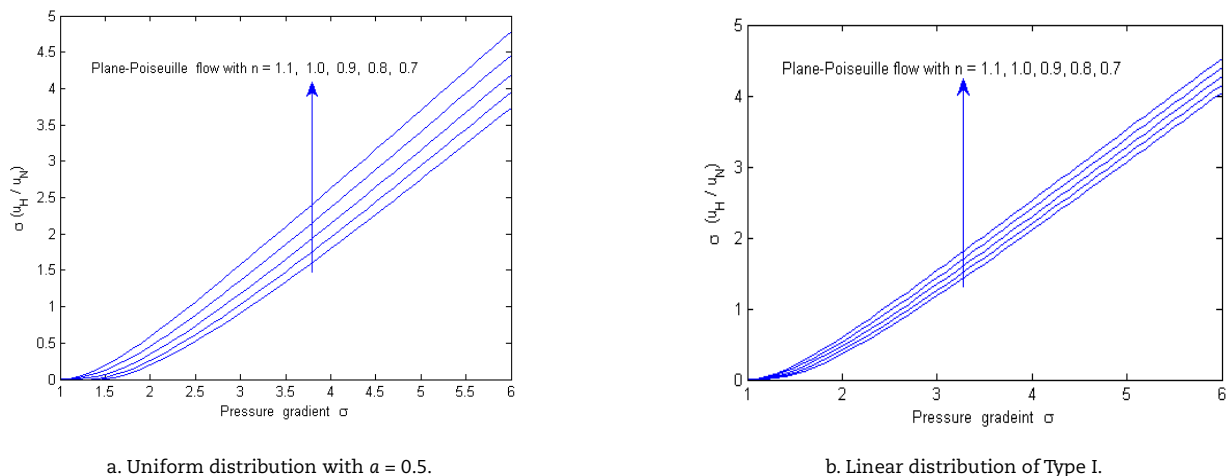
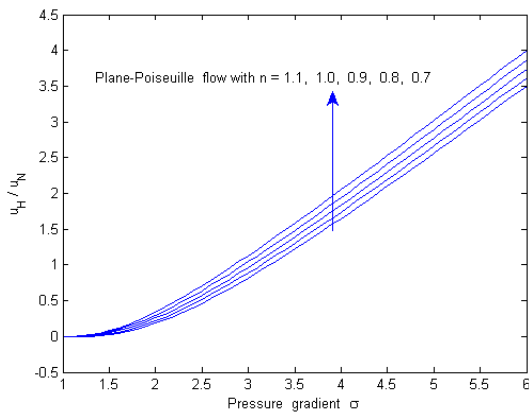


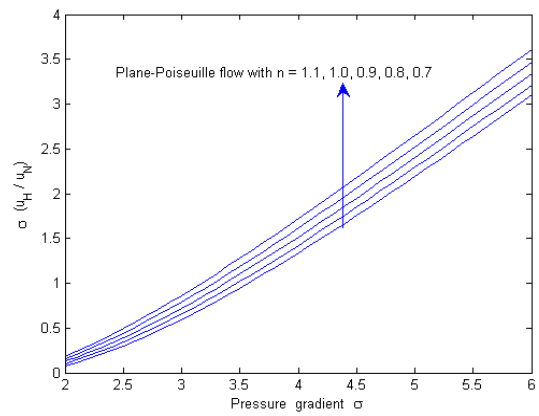
Fig. 7. Variation of mean velocity with pressure gradient in plane-Poiseuille flow for distinct values of the parameter n when the channel widths are represented by different probability density functions.

The variation of dimensionless mean velocity with pressure gradient in flow through channel for various values of the parameter n when the channels distribution in the porous flow medium are represented by four types of probability density functions (a. Uniform distribution with $a = 0.5$; b. Linear distribution of Type-I; c. Linear distribution of Type-II and d. Quadratic distribution) is plotted in Fig. 8. It is seen that in all the four types of the pores distribution, dimensionless mean velocity increases slowly when the pressure gradient raises from 1 to 2 and then it soars up with the rise of pressure gradient from 2 to 6. The dimensionless mean velocity is higher (by 5.25%) when the pores in the flow medium are dispersed in uniform distribution than when the pores in the flow medium follow linear distribution of type I. It is clear that the dimensionless mean velocity is higher (by 10.5%) when the pores scattering follow linear distribution of type I than when the pores distribution follow linear distribution of type II. It is further recorded that the dimensionless mean velocity is higher (by 10%) when the pores are distributed in the linear distribution of type II than when the pores of the flow medium are distributed in quadratic distribution. One can also notice that the dimensionless mean velocity increases slightly when the parameter n increases which exhibits the non-Newtonian character of H-B fluid.



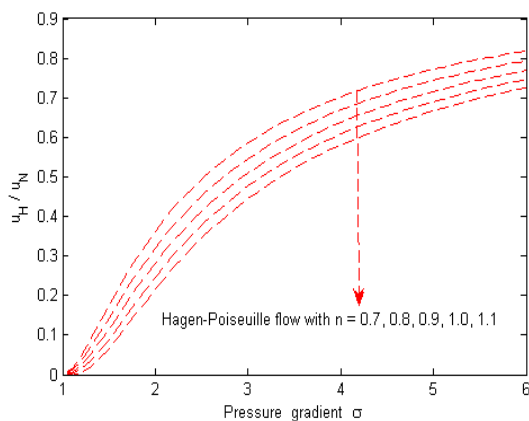


c. Linear distribution of Type II.

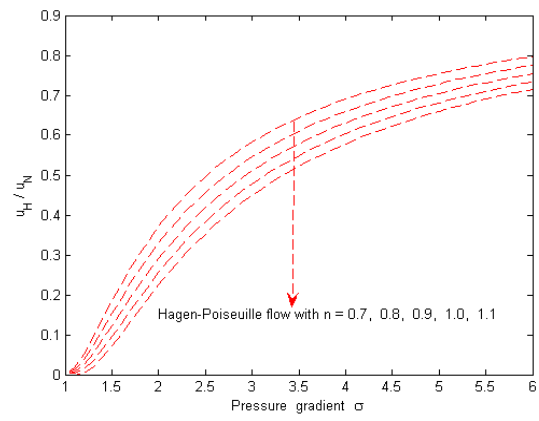


d. Quadratic distribution.

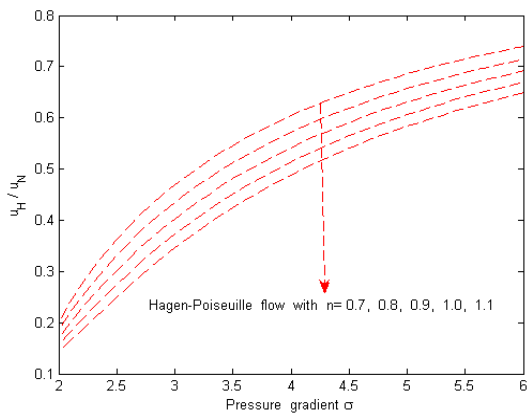
Fig. 8. Variation of dimensionless mean velocity with pressure gradient in plane-Poiseuille flow for distinct values of the parameter n when the channel widths are represented by different probability density functions.



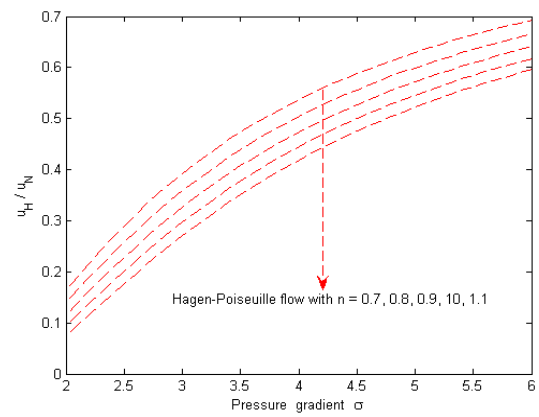
a. Uniform distribution with $\alpha = 0.5$.



b. Linear distribution of Type-I.



c. Linear distribution of Type-II.



d. Quadratic distribution.

Fig. 9. Variation of mean velocity with pressure gradient in Hagen-Poiseuille flow for distinct values of the parameter n when the pores are represented by different probability density functions.

Fig. 9 sketches the variation in the mean velocity with respect to pressure gradient in Hagen-Poiseuille flow for distinct power law index n values when pores in the porous flow medium follow four different kinds of probability density functions. (a. Uniform distribution with $\alpha = 0.5$; b. Linear distribution of Type-I; c. Linear distribution of Type-II and d. Quadratic distribution). The kinds of variation in mean velocity (with respect to pressure gradient and power law index for the four types of pores width distribution) that are observed in Fig. 9 are very similar to the variations in mean velocity (with respect to the same set of parameters) which are recorded in Fig. 7. The variation in the dimensionless mean velocity with respect to the pressure gradient in Hagen-Poiseuille flow for distinct values of power law index parameter n values when the pores distribution are represented by four different types probability density functions (a. Uniform distribution with $\alpha = 0.5$; b. Linear distribution of Type-I; c. Linear distribution of Type-II and d. Quadratic distribution). The nature of variation in mean velocity (with respect to pressure gradient and power law index for the four types of pores width distribution) which are observed in Fig. 8 are also seen in the variations of fluid's Darcy mean velocity (with respect to the same set of parameters) in Fig. 10.



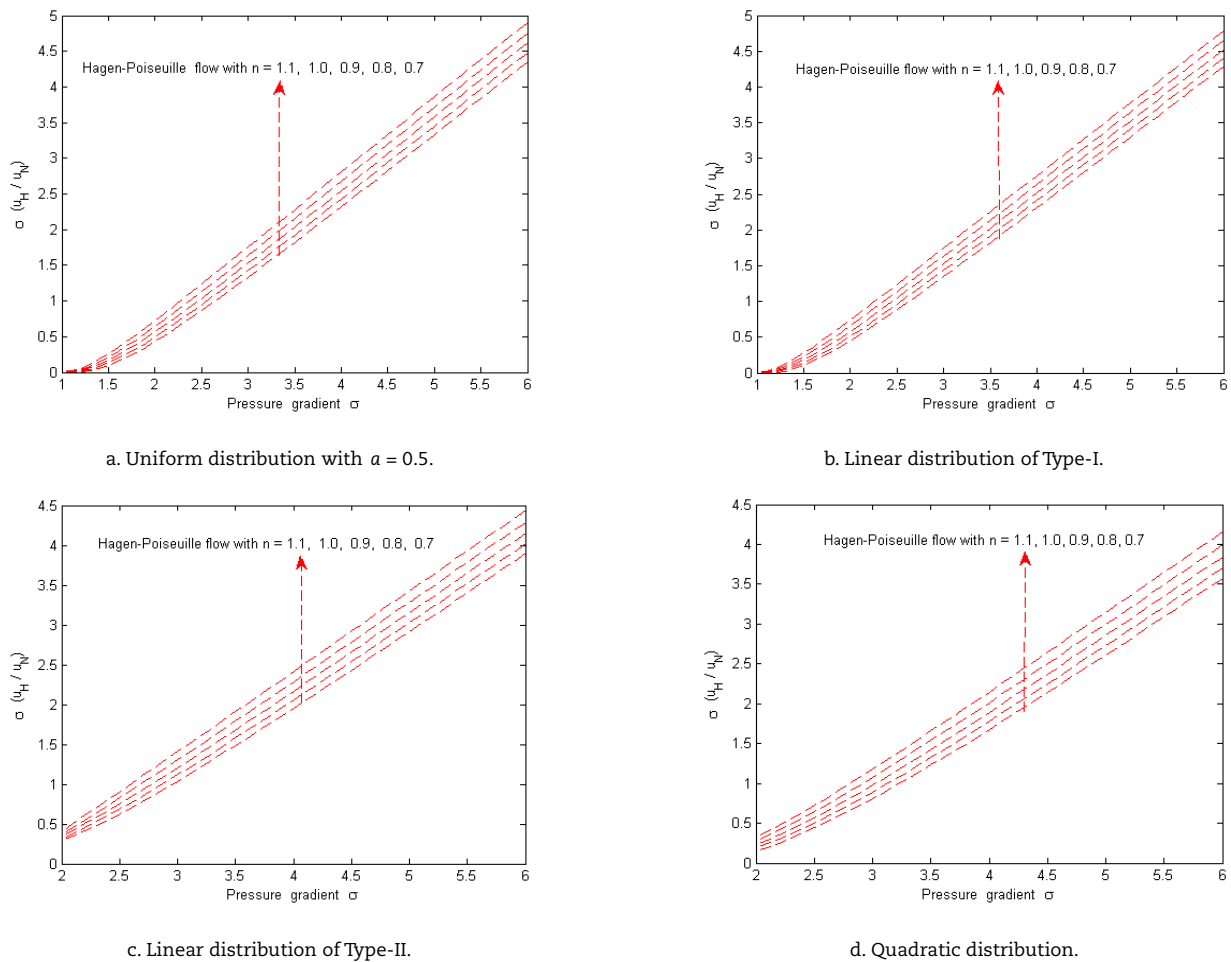


Fig. 10. Variation of dimensionless mean velocity with pressure gradient in Hagen-Poiseuille flow for distinct values of the parameter n when the pores are represented by different probability density functions.

3.5 Porosity of the flow medium

Fig. 11 depicts the variation in porosity with respect to period of channels/pipes when the pores in the pipes/channels are distributed in uniform distribution with $h = 0.7$. It is clear that the flow medium's porosity descends rapidly with the raise of the period of pipes/channels from 1 to 2 and then it descends very slowly (almost constant) with the further increase of the period of channels from 2 to 11. One can also notice that the porosity in the flow medium increases slightly with the raise of uniform distribution parameter 'a' when rest of the parameters were treated as invariables. When all the flow parameters are treated as invariable, the flow medium's porosity is slightly higher in flow through circular pipe than in flow in rectangular channel when the period of the pipes/channels lies between (i) 1 and 1.6 when $a = 0.2$, (ii) 1 and 1.8 when $a = 0.4$, (iii) 1 and 2.0 when $a = 0.6$ and (iv) 1 and 2.2 when $a = 0.8$ and this behavior is reversed when the period of the pipes/channels lies from the respective end point of each of the aforesaid four cases until $H = 11$.

The variation of porosity with period of channels in H-B fluid flow for different radii of pipes (Hagen-Poiseuille flow) and distinct width of channels (plane-Poiseuille flow) when the pores in the flow medium represented by four kinds of probability density functions is shown in Fig. 12 [(a) Uniform distribution with $a = 0.8$, (b) Linear distribution of Type-I, (c) Linear distribution of Type-II and (d) Quadratic distribution]. One can further observe that the porosity of the flow medium decreases with the rise of the period of pipes/channels from 1 to 2 and then it descends very slowly with the raise of the period of channels from 2 to 11. It is further noted that the porosity of the flow medium increases marginally when the radii of pipes/width of channels increase. For a set of fixed values of all the parameters, the porosity of the flow medium with uniformly distributed pores is significantly higher than the porosity of the flow medium with pores scattered in linear distribution of type I which is considerably higher than the porosity of the flow medium with quadratically distributed pores.

Table 1 computes the range of period of pipes/channels H where porosity is higher in flow through circular pipes than in flow through rectangular channels when the pores of the flow medium are represented by different probability density functions. Table 2 presents the range of period of pipes/channels H where porosity is substantially higher in flow through channels than in flow through circular pipes when the pores in the flow medium are modelled by three probability density functions.

Table 1. Range of period of pipes/channels H where porosity is higher in Hagen-Poiseuille flow than in plane-Poiseuille flow when the pores in the flow medium are represented by in different probability density functions.

Radii of pipes/width of channels h	Uniform distribution	Linear distribution of type I	Linear distribution of type II	Quadratic distribution
0.6	1 – 1.6	1 – 1.4	No range exists	No range exists
0.7	1 – 2	1 – 1.7	No range exists	No range exists
0.8	1 – 2.35	1 – 2	1 – 1.3	1 – 1.2
0.9	1 – 2.7	1 – 2.25	1 – 1.7	1 – 1.4
1	1 – 2.95	1 – 2.5	1 – 1.95	1 – 1.6



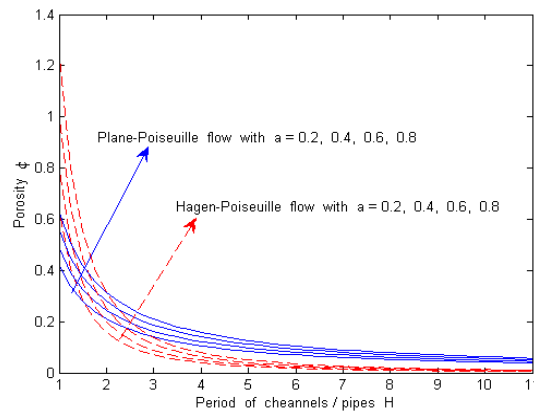
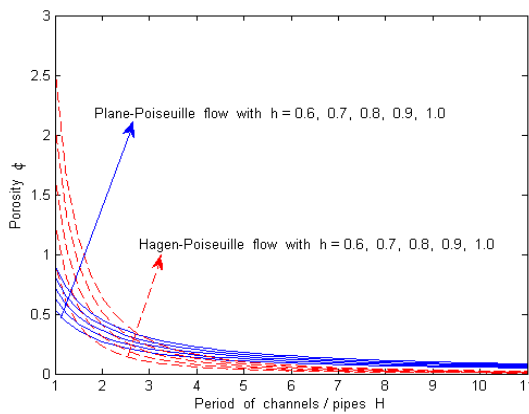
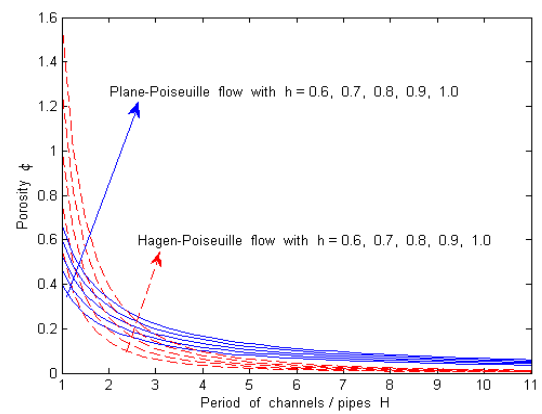


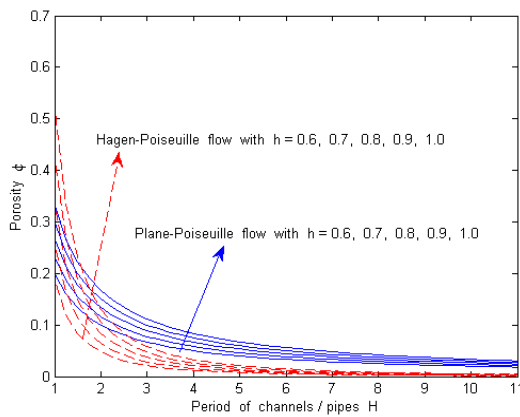
Fig. 11. Variation of Porosity with period of channels/pipes when they are distributed in uniform distribution with $h = 0.7$.



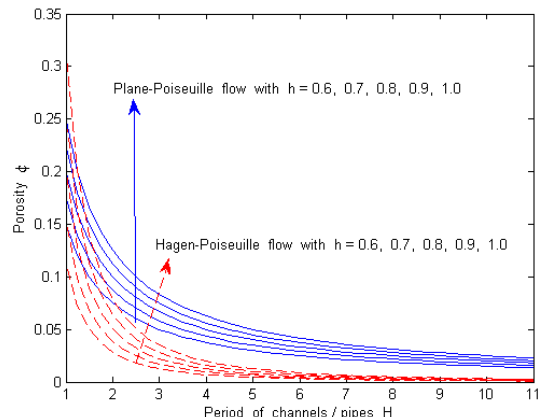
a. Uniform distribution with $a = 0.8$.



b. Linear distribution of Type-I.



a. Uniform distribution with $a = 0.5$.



b. Linear distribution of Type-I.

Fig. 12. Variation of Porosity with period of channels for distribution of channels / pipes by various probability density functions.

Table 2. Range of period of pipes/channels H where porosity is higher in plane-Poiseuille fluid flow than in Hagen-Poiseuille flow when the pores in the flow medium are represented by in different probability density functions.

Radii of pipes/width of channels h	Uniform distribution	Linear distribution of type I	Linear distribution of type II	Quadratic distribution
0.6	1.6 – 11	1.4 – 11	1 – 11	1 – 11
0.7	2 – 11	1.7 – 11	1 – 11	1 – 11
0.8	2.35 – 11	2 – 11	1.3 – 11	1.2 – 11
0.9	2.7 – 11	2.25 – 11	1.7 – 11	1.4 – 11
1.0	2.95 – 11	2.5 – 11	1.95 – 11	1.6 – 11



3.6 Permeability of the flow medium

Fig. 13 plots the variation of permeability with period of pipes/channels when the pore in the flow medium are represented by uniform distribution for distinct values of its parameter 'a' with $n = h = 0.7$. For plane-Poiseuille flow, the permeability of the porous flow medium decreases quickly with the upraise of the period of channels from 1 to 2 and then it reduces very slowly (almost constant) with the increase of the period of channels in the flow medium from 2 to 11, whereas in Hagen-Poiseuille flow, the permeability of the porous flow medium descends rapidly with the upraise of the period of pipes from 1 to 3 and then it descends very slow when the period of pipes increases from 3 to 11. It is also recorded that the permeability of the flow medium is substantially higher in flow through circular pipes than in flow through rectangular channels when the period of the pipes/channels lies between 1 and 2.45 when $a = 0.2$, 1 and 2.60 when $a = 0.4$, 1 and 2.75 when $a = 0.6$, 1 and 2.90 when $a = 0.8$ and this behavior is reversed when the period of the pipes/channels lies between 2.45 and 11 when $a = 0.2$, 2.60 and 11 when $a = 0.4$, 2.75 and 11 when $a = 0.6$ and, 2.90 and 11 when $a = 0.8$.

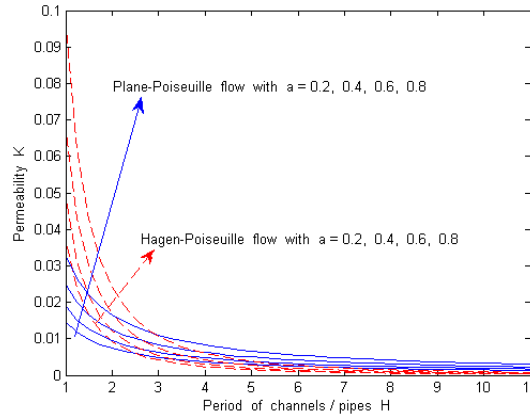
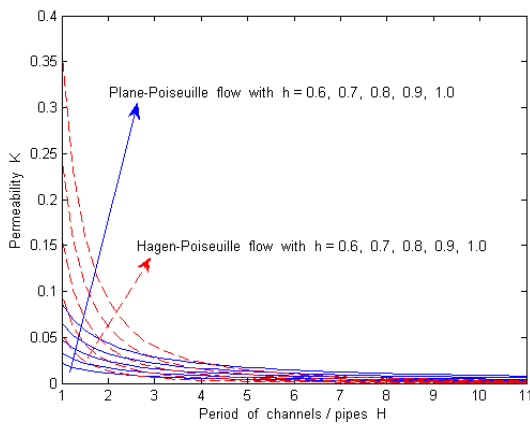
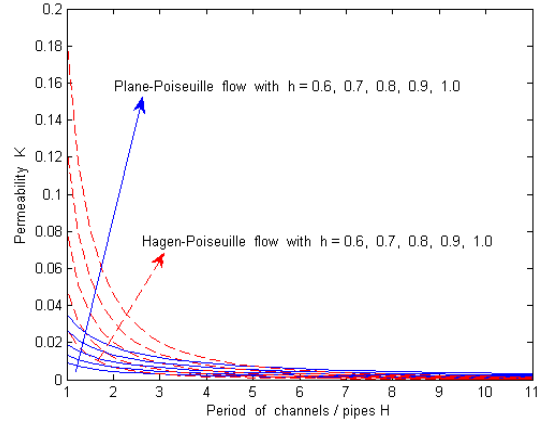


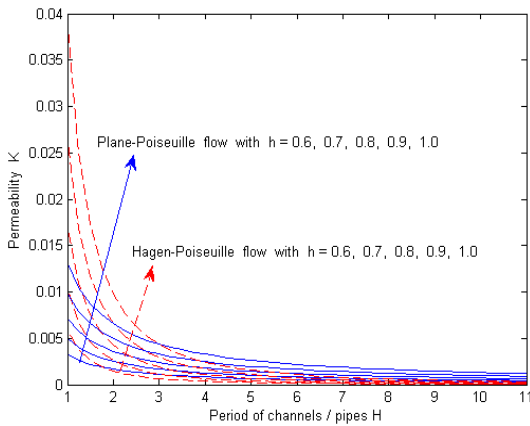
Fig. 13. Variation of permeability with period of pipes/channels when the distribution of pores in the flow medium is represented by uniform distribution for different values its parameter 'a' with $n = h = 0.7$.



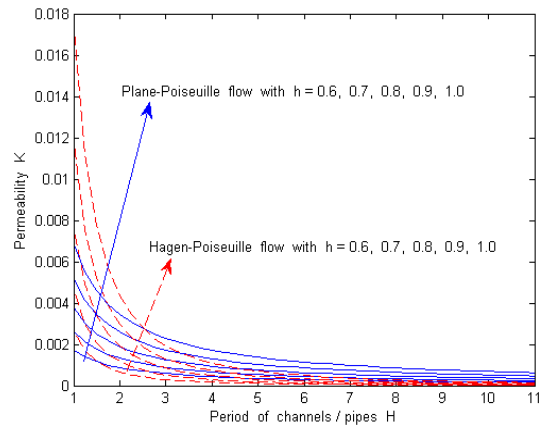
a. Uniform distribution.



b. Linear distribution of Type-I.



c. Linear distribution of Type-II.



d. Quadratic distribution.

Fig. 14. Variation of permeability with period of pipes/channels when the distribution of pores in the flow medium is represented by four kinds of probability density functions and for different values of multi-pipes radii/multi-channels width with $n = 0.7$.



Table 3. Range of period of pipes/channels H where permeability is higher in Hagen-Poiseuille fluid flow than in plane-Poiseuille flow when the pores in the flow medium are represented by in different probability density functions.

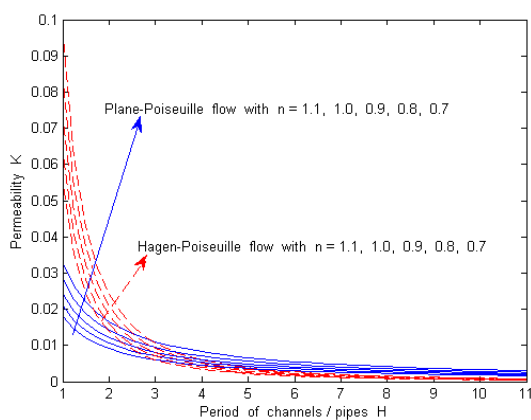
Radii of pipes/width of channels h	Uniform distribution	Linear distribution of type I	Linear distribution of type II	Quadratic distribution
0.6	1 – 2.25	1 – 2.5	1 – 1.75	1 – 1.5
0.7	1 – 2.75	1 – 2.75	1 – 2	1 – 1.75
0.8	1 – 2.50	1 – 3	1 – 2.25	1 – 2
0.9	1 – 3.75	1 – 4	1 – 2.75	1 – 2.25
1	1 – 4	1 – 4.50	1 – 3	1 – 2.50

Table 4. Range of period of pipes/channels H where porosity is higher in flow through channels circular artery than in flow through circular plane when the pores in the flow medium are represented by in different probability density functions.

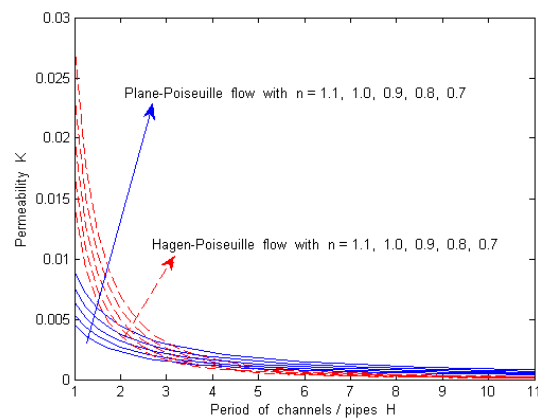
Radii of pipes/width of channels h	Uniform distribution	Linear distribution of type I	Linear distribution of type II	Quadratic distribution
0.6	2.25 – 11	2.50 – 11	1.75 – 11	1.50 – 11
0.7	2.75 – 11	2.75 – 11	2 – 11	1.75 – 11
0.8	2.50 – 11	3 – 11	2.25 – 11	2 – 11
0.9	3.75 – 11	4 – 11	2.75 – 11	2.25 – 11
1.0	4 – 11	4.50 – 11	3 – 11	2.50 – 11

The variation in permeability with respect to the period H of pipes/channels for different radii of pipes (Hagen-Poiseuille flow) and distinct width of channels (plane-Poiseuille flow) when the pores in the flow medium are modelled by four kinds of probability density functions with $n = 0.7$, is illustrated in Figs. 14 (i) – 14 (iv) [(i) Uniform distribution with $a = 0.8$, (ii) Linear distribution of Type-I, (iii) Linear distribution of Type-II and (iv) Quadratic distribution]. It is found that the permeability of the flow medium decreases with the rise of the period of pipes/channels from 1 to 2 and then it reduces very slowly with the raise of the period of channels from 2 to 11. It is also clear that the flow medium's permeability ascend marginally with the increase of the radii of pipes/width of channels. Table 3 computes the range of period of pipes/channels H where the permeability of the flow medium is higher in flow through circular pipes than in flow through channels when the pores in the flow medium are represented by any of the four kinds of probability density functions. Table 4 presents the range of period of pipes/channels H where permeability is higher in flow through pipes than flow in channels when the pores in the flow medium are represented by in different probability density functions. When all of the rheological parameters are held as invariable, the permeability of the flow medium with uniformly scattered pores is significantly higher than the permeability of the flow medium with pores dispersed in linear distribution of type I which is considerably higher than the permeability of the flow medium with pores distributed in linear distribution of type II which in turn is marginally higher than the permeability of the flow medium with quadratically distributed pores.

Figs. 15 (i) – 15 (iv) depict the variation in permeability of flow medium with respect to the period H of pipes/channels for distinct values of non-Newtonian power law index parameter n when the pores in the flow medium are modelled by four types of probability density functions with $h = 0.7$. [(i) Uniform distribution with $a = 0.8$, (ii) Linear distribution of Type-I, (iii) Linear distribution of Type-II and (iv) Quadratic distribution]. In plane-Poiseuille fluid flow, the permeability of the flow medium decreases rapidly with the rise of the period of pipes/channels from 1 to 2 and then it reduces very slowly when the period of channels ascends from 2 to 11, whereas in Hagen-Poiseuille fluid flow past the porous flow medium, the flow medium's permeability slumps with the rise of the flow period of pipes/channels, the from 1 to 3 and then it decreases very slowly (is almost constant). One can also notice that the permeability of the flow medium descends marginally when the power law index parameter n increases. Table 3 estimates the range of period of pipes/channels H where permeability is higher in Hagen-Poiseuille flow than in plane-Poiseuille flow when the pores in the flow medium are represented by the aforesaid four probability density functions. Table 4 presents the range of period of pipes/channels H where permeability is higher in plane-Poiseuille flow than in Hagen-Poiseuille fluid flow when the pores in the flow medium are represented by different probability density functions. For a set of fixed values of rheological parameters, the permeability of the flow medium is significantly higher when the pores are uniformly dispersed than when the pores spread out in linear distribution of type I which is considerably higher than the permeability of the flow medium with pores scattered in linear distribution of type II which in turn is marginally higher than the permeability of the flow medium with quadratically sprinkled pores.



a. Uniform distribution.



b. Linear distribution of Type-I.



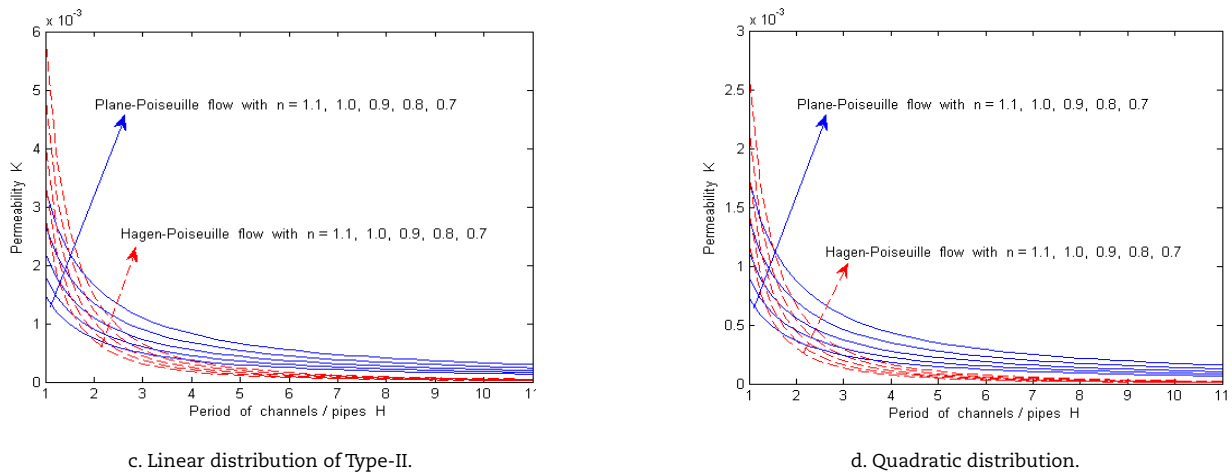


Fig. 15. Variation of permeability with period of pipes/channels when the distribution of pores in the flow medium is represented by four kinds of probability density functions and for different values of the parameter n with $n = 0.7$.

Table 5. Range of period of pipes/channels H where permeability is higher in Hagen-Poiseuille fluid flow than in plane-Poiseuille flow when the pores in the flow medium are represented by in distinct probability density functions.

Power law index n	Uniform distribution	Linear distribution of type I	Linear distribution of type I	Quadratic distribution
0.7	1 – 2.90	1 – 3.2	1 – 1.65	1 – 1.50
0.8	1 – 2.93	1 – 3.15	1 – 1.70	1 – 1.55
0.9	1 – 2.97	1 – 3.10	1 – 1.75	1 – 1.60
1	1 – 3.02	1 – 3.05	1 – 1.80	1 – 1.65
1.1	1 – 3.08	1 – 3.00	1 – 1.85	1 – 1.70

Table 6. Range of period of pipes/channels H where porosity is higher in plane-Poiseuille fluid flow than in Hagen-Poiseuille flow when the pores in the flow medium are represented by in distinct probability density functions.

Power law index n	Uniform distribution	Linear distribution of type I	Linear distribution of type II	Quadratic distribution
0.7	2.90 – 11	3.20 – 11	1.65 – 11	1.50 – 11
0.8	2.93 – 11	3.15 – 11	1.70 – 11	1.55 – 11
0.9	2.97 – 11	3.10 – 11	1.75 – 11	1.60 – 11
1.0	3.02 – 11	3.05 – 11	1.80 – 11	1.65 – 11
1.1	3.08 – 11	3.00 – 11	1.85 – 11	1.70 – 11

From Figs. 11 – 15, it is found that the porous medium’s permeability and porosity are flow through circular pipes has in flow through significantly higher when the pores distribution in the flow medium follow linear distribution of type I than when pores distribution follows the linear distribution of Type-II. This character is exhibited due to the fact that the gradient $d\psi/d\gamma$ of the type I and type II of the linear distribution of pores are positive and negative respectively (i.e., the pore size increases with the rise of the pipes radii ratio / channels widths ratio parameter γ in linear distribution of type I, while it reduces with γ in linear distribution of type II). Hence, for a fixed value of γ , the pore size in linear distribution of type I is larger than that in linear distribution of type II, thus the permeability and porosity of flow medium in Type II of linear distribution of pores are quite lower than those in Type I of linear distribution of pores.

3.7 Discussion on the results

From the results of plotted graphs and computed data in tables, one can have more insightful physical understanding on the flow characteristics of H-B fluid in porous flow media when the flow is assumed as (i) plane-Poiseuille flow and (ii) Hagen-Poiseuille flow and when the size of pores in the flow medium are assumed to follow the three different kinds of distribution, as discussed in this section.

From Figs. 3(a) and 3(b), one can realize that the flow rate of H-B fluid flow raises monotonically with the rise of pressure gradient of flow and flow rate is marginally higher in Hagen-Poiseuille flow than in the plane-Poiseuille flow. This implies that the permeability and porosity of the porous flow medium with circular pores is marginally lower than that with rectangular pores. From Figs. 4 - 6, it is observed that in both plane-Poiseuille flow and Hagen-Poiseuille flow in single/multi channel/pipe flow, the Darcy mean velocity raises rapidly with the increase of the pressure gradient up to 2.5 and thereafter it rises slowly with the further rise of the pressure gradient up to 5, which means that up to the pressure gradient level of 2.5, the porosity and permeability in the fluid flow are yet to reach the peak and they raises with the further rise of the pressure gradient till 5. From Figs. 7 – 10, we note that in all kinds of probability distribution of pores sizes, the Darcy mean velocity is considerably higher in Hagen-Poiseuille flow than in plane-Poiseuille flow, meaning that the effects of porosity and permeability are considerably higher in flow through porous with medium with rectangular pores than with circular pores, i.e., the flow in porous medium with circular pores considerably reduces the loss of fluid transport than in porous flow medium with rectangular pores.

Figs. 11 – 15 exhibits that the porosity and permeability of the porous medium decreases significantly with the increase of the period of channels/pipes from 1 to 2.5 and then they decrease when the period of channels/pipes rises from 2.5 to 11. This means, the effects of porosity and permeability of the porous medium decreases considerably when the size of the pores decreases and thus loss of fluid during the flow can be significantly reduced by enhancing the period of channels/pipes (i.e., reducing the radii of circular pores/width of rectangular pores). It is also noted that among the four probability distribution of pores sizes, the porosity and permeability of the porous medium are highest when the pores sizes follows linear distribution of type I (increasing function of scaling factor γ) and lowest when the pores sizes follow quadratic distribution (decreasing function of scaling factor γ). This implies that for a greater and lesser impact of porosity and permeability, one can model the sizes of the pores in the flow medium by linear distribution of type I and quadratic distribution respectively.



4. Conclusions

This theoretical study investigates the effects of several flow parameters on the flow measurements in the plane-Poiseuille and Hagen-Poiseuille flows of H-B fluid in a porous medium which is composed of (i) single pipe/channel and (ii) multi-pipes/multi-channels when the pores in the multi-pipes/multi-channels are represented by any one of the following four types of probability density functions: (i) Uniform distribution, (ii) Linear distribution of Type-I, (iii) Linear distribution of Type-II and (iv) Quadratic distribution. The major outcomes of this mathematical investigation are listed hereunder:

- In both plane-Poiseuille and Hagen-Poiseuille flows, the Buckingham-Reiner function (flow rate) increases linearly with the rise of pressure gradient from 1 to 2.5 and then it increases very slowly with the further raise of the pressure gradient from 2.5 to 5.
- When the pressure gradient is held constant, the Darcy mean velocity and Buckingham-Reiner function are considerably higher in flow through pipes than in flow through channels.
- With the rise of the pressure gradient, the mean velocity increases almost linearly in flow through channel flow; whereas in the case of flow through circular pipes) when the pressure gradient increases.
- The Darcy mean velocity, permeability and porosity of the flow medium ascends considerably with the rise of the pipe radius/channel width.
- The Darcy mean velocity, permeability and porosity of the flow medium increases considerably when the uniform distribution parameter a raises.
- The porosity of the flow medium decreases rapidly with the rise of the period H of the pipes/ channels distribution from 1 to 2 and it drops very slowly with the further rise of the period of the pipes/channels H from 2 to 11.
- The flow medium's permeability and porosity are significantly higher when the pores in the flow medium follow uniform distribution than when pores in the flow medium are dispersed in linear distribution of type I which is markedly higher when the pores are distributed in linear distribution of type II which is considerably higher than to those when the pores of the flow medium are distributed in quadratic distribution.
- The Darcy mean velocity, permeability and porosity of the flow medium descends marginally when the power law index parameter increases which signifies the non-Newtonian characteristics of this fluid model

From the results discussed in this mathematical analysis, it is hoped that this theoretical investigation would provide a good insight to the reader about the flow characteristics of non-Newtonian fluids' flow in a porous medium in which the dispersion of pores are represented by four different types of probability density functions. It is also expected that the present theoretical study would propel the readers to pursue advanced research in this research area to find out more new results which would be useful to the relevant industry. The study about fluid flow in porous medium by the pore scale approach has two phases from the methodological aspects. The first phase is to apply the macroscopic techniques to measure and analyze the integrated three-dimensional information on pore-scale microstructure and the second phase is to make use of predictive micro-modelling to develop the deep understanding of the heat and mass transfer in complex pores for exploring the underlying transport mechanism in porous medium. Since the pore scale approach would yield more realistic and useful information on fluid flow in porous medium, it would be taken up in our immediate future study.

Author Contributions

D.S. Sankar perceived the research problem, formulated it as mathematical model and contributed in obtaining the analytical solutions, analyzing the results and revising the manuscript as commented by the reviewers and editor. K.K. Viswanathan contributed in obtaining the expressions for rheological quantities and involved in generating the data for plotting the graphs through MATLAB programming. Atulya K. Nagar involved in analyzing the results obtained through the graphical and tabular representation of data. Nurul Aini Binti Jafaar contributed in collecting the relevant literature and validating the results. A. Vanav Kumar contributed in MATLAB programming, writing the manuscript and then in revising it as suggested by the reviewers. All the authors contributed in the manuscript preparation. All authors discussed the results, reviewed and approved the final version of the manuscript.

Acknowledgement

The authors thank the editor and reviewer for their constructive comments which significantly improved the scientific value of the research article.

Conflict of Interest

The authors declared no potential conflicts of interest with respect to the research, authorship and publication of this article.

Funding

The authors received no financial support for the research, authorship and publication of this article.

Data Availability Statements

The datasets generated and/or analyzed during the current study are available from the corresponding author on reasonable request.

Nomenclature

Upper alphabetical symbols

- F Darcy velocity u_H/u_N in plane-Poiseuille flow (dimensionless)
 G Darcy velocity u_H/u_N in Hagen-Poiseuille flow (dimensionless)

Upper Greek Symbols

- Ω Negative of the pressure gradient $[N/m^2]$

Lower Greek Symbols



H	Period of the pattern of channels/pipe [$1/m^2$]	\in	Unyielded portion of the pipe/channel [m]
K	Permeability of the flow medium [N/m^2]	ϕ	Porosity of flow medium (dimensionless)
N	Number of channel/pipes	γ	Channel width/ pipe radius relative to h [m]
Q	Volumetric flow rate in channel/pipe [m^3/s]	μ	Dynamic viscosity [Ns/m^2]
Lower alphabetical letters		τ	Shear stress [N/m^2]
a	Parameter associated with the uniform distribution (dimensionless)	τ_y	Yield stress [N/m^2]
f	Buckingham-Reiner function for plane-Poiseuille flow (dimensionless)	Subscript symbols	
g	Buckingham-Reiner function for Hagen-Poiseuille flow (dimensionless)	H	Herschel-Bulkley fluid
h	Width/radius of the channel/pipe [m]	N	Newtonian fluid
p	Pressure in the fluid flow through channel/pipe [N/m^2]	pt	Pseudo-thresholds of stress
u_H	Axial velocity of Herschel-Bulkley fluid [m/s]	y	Yield stress
u_N	Axial velocity of Newtonian fluid [m/s]		
r	Radial coordinate in polar coordinates [m]		
x	Axial coordinate in Cartesian coordinates [m]		
y	Vertical coordinate in Cartesian coordinates [m]		

Appendix

Hagen-Poiseuille flow of H-B fluid

A. H-B fluid flow in a porous circular pipe

Consider the Hagen-Poiseuille flow of H-B fluid in a circular tube/pipe of uniform radius h . The volumetric flow rate of H-B fluid in a single pipe (analogous to that of Eq. (6a)) is

$$Q = 2\pi \int_0^h u dr = 2 \left[\int_0^{\epsilon h} r u_p dr + \int_{\epsilon h}^h r u dr \right] = \frac{8\pi \Omega^n}{(n+3)\mu} \left(\frac{h}{2} \right)^{n+3} g(\sigma), \quad (\text{A.1})$$

where

$$g(\sigma) = \begin{cases} 1 - \frac{n(n+3)}{(n+2)|\sigma|} + \frac{n(n-1)(n+3)}{2(n+1)|\sigma|^2} - \frac{(n^4 + 2n^3 - 5n^2 - 6n + 4)}{2(n+1)(n+2)|\sigma|^{n+3}} & \text{if } |\sigma| > 1 \\ 0 & \text{if } |\sigma| < 1 \end{cases} \quad (\text{A.2})$$

The function $g(\sigma)$ given in Eq. (A.2) is the Buckingham-Reiner function (formula) for the laminar and steady flow of H-B fluid in a circular pipe. The Darcy velocity u_H of H-B fluid flow in porous circular tubes is obtained as below:

$$u_H = \frac{2\varphi \Omega^n}{(n+3)\mu} \left(\frac{h}{2} \right)^{n+1} g(\sigma) = \frac{\Omega^n K}{\mu} g(\sigma), \quad (\text{A.3})$$

where

$$\varphi = \frac{\pi h^2}{H^2} \quad \text{and} \quad K = \frac{2\varphi}{(n+3)} \left(\frac{h}{2} \right)^{n+1}. \quad (\text{A.4,5})$$

When $\sigma \gg 1$, the normalized mean velocity $g(\sigma)$ of H-B fluid flow simplifies to the quadratic form given below:

$$g(\sigma) = \frac{1}{2}(n-2)(n-1)(n+3)(\sigma-1) - \frac{1}{4}(n-2)(n+3)(n^2+5n-4)(\sigma-1)^2 + \frac{1}{12}(n+3)(n^4+8n^3+7n^2-72n+40)(\sigma-1)^4 + \dots, \quad 0 < (\sigma-1) \ll 1 \quad (\text{A.6})$$

For quite large values of σ ($\sigma \gg 1$), Buckingham-Reiner formula Eq. (A.2) reduces to the two-term approximation as given in Eq. (A.7):

$$\sigma g(\sigma) \approx \sigma - \frac{n(n+3)}{(n+2)} \quad (\text{A.7})$$

B. H-B fluid rheology in a porous flow medium with two pipes of different radii

The total rate of flow of H-B fluid flow in one period of pipes which consists of a wider tube of radius h and a narrow tube of radius γh , ($\gamma < 1$) is defined by the following formula [Nash and Rees, 40]:

$$Q = \frac{8\pi \Omega^n}{(n+3)\mu} \left(\frac{h}{2} \right)^{n+3} [g(\sigma) + \gamma^{n+3} g(\gamma\sigma)]. \quad (\text{B.1})$$

The Darcy velocity of H-B fluid flow is



$$u_H = \frac{\Omega^n K}{\mu} \left(\frac{g(\sigma) + \gamma^{n+3} g(\gamma\sigma)}{1 + \gamma^{n+3}} \right), \tag{B.2}$$

where

$$K = \frac{2\varphi(1 + \gamma^{n+3})}{(1 + \gamma^2)} \left(\frac{h}{2} \right)^{n+1} \quad \text{and} \quad \varphi = \pi(1 + \gamma^2) \left(\frac{h}{H} \right)^2, \tag{B.3}$$

are respectively the flow medium’s permeability and porosity. The normalized mean velocity of H-B fluid flow relative to that of Newtonian fluid flow is

$$u_H/u_N = G(\sigma) = \frac{g(\sigma) + \gamma^{n+3} g(\gamma\sigma)}{(1 + \gamma^{n+3})} \tag{B.4}$$

For quite large values of $\sigma (\sigma \gg 1)$, the normalized mean velocity (B.4) reduces to the following form:

$$\sigma g(\sigma) \approx \sigma - \frac{n(n+3)(1 + \gamma^{n+2})}{(n+2)(1 + \gamma^{n+3})}. \tag{B.5}$$

From Eq. (B.5), one can obtain the pseudo-threshold value of the pressure gradient for this kind of flow as

$$\sigma_{pt} \approx \frac{n(n+3)(1 + \gamma^{n+2})}{(n+2)(1 + \gamma^{n+3})}. \tag{B.6}$$

C. H-B fluid flow through porous medium with several pipes of different radii

For the H-B fluid flow in a porous medium which is composed of multi-tubes of radii $\gamma_i h, i = 1, 2, \dots, N$, the Darcy velocity of H-B fluid in relation to Newtonian fluid, porosity and permeability of the flow medium are obtained as in Eqs. (A14) – (A16) respectively.

$$u_H/u_N = G(\sigma) = \left[\frac{\sum_{i=1}^N \gamma_i^{n+3} g(\gamma_i \sigma)}{\sum_{i=1}^N \gamma_i^{n+3}} \right], \tag{C.1}$$

$$K = \frac{2\varphi}{(n+3)} \left(\frac{h}{2} \right)^{n+1} \left[\frac{\sum_{i=1}^N \gamma_i^4}{\sum_{i=1}^N \gamma_i^2} \right] \quad \text{and} \quad \varphi = \pi \left(\frac{h}{H} \right)^2 \sum_{i=1}^N \gamma_i^2. \tag{C.2,3}$$

For large values of $\sigma (\sigma \gg 1)$, the normalized mean velocity (C.1) reduces to the following form:

$$\sigma g(\sigma) \approx \sigma - \frac{n(n+3)}{(n+2)} \left[\frac{\sum_{i=1}^N \gamma_i^{n+2}}{\sum_{i=1}^N \gamma_i^{n+3}} \right]. \tag{C.4}$$

From Eq. (C.4), we get the pseudo-threshold value of the pressure gradient for this kind of flow as

$$\sigma_{pt} = \frac{n(n+3)}{(n+2)} \left[\frac{\sum_{i=1}^N \gamma_i^{n+2}}{\sum_{i=1}^N \gamma_i^{n+3}} \right] \tag{C.5}$$

D. Simulating the distribution of pores by probability density functions

When the continuous probability density functions $\psi(\gamma)$ are applied to model the distribution of radii of circular pipes in porous medium, then the Darcy velocity of fluid flow, permeability and porosity of the flow medium are obtained by using Eqs. (D.1) – (D.3) respectively [40]:

$$G(\sigma) = \frac{u_H}{u_N} = \frac{\int_0^\infty \gamma^{n+3} \psi(\gamma) g(\gamma\sigma) d\gamma}{\int_0^\infty \gamma^{n+3} \psi(\gamma) d\gamma}, \tag{D.1}$$

$$K = \frac{2\varphi}{(n+3)} \left(\frac{h}{2} \right)^{n+1} \frac{\int_0^\infty \gamma^{n+3} \psi(\gamma) d\gamma}{\int_0^\infty \gamma^2 \psi(\gamma) d\gamma}, \tag{D.2}$$

$$\varphi = \pi \left(\frac{h}{H} \right)^2 \int_0^\infty \gamma^2 \psi(\gamma) d\gamma. \tag{D.3}$$

(i) Uniform probability distribution

When the widths of the pores of circular pipes in the porous medium are represented by the density function of uniform probability distributed (as given in Eq. (27)), the analytical solutions to the normalized Darcy mean velocity, permeability and porosity of the porous flow medium are obtained as Eqs. (D.4) – (D6) respectively:



$$G(\sigma) = \begin{cases} 0 & \text{if } 0 \leq \sigma < 1 \\ \frac{\left\{ \begin{aligned} &2(n+1)(n+2)\sigma^{n+4} - 2n(n+1)(n+4)\sigma^{n+3} + n(n-1)(n+3)(n+4)\sigma^{n+2} \\ &-(n+4)(n^4 + 2n^3 - 5n^2 - 6n + 4)\sigma + (n^5 + 5n^4 - n^3 - 23n^2 - 6n + 12) \end{aligned} \right\}}{2(n+1)(n+2)(n+4)(1-a^{n+4})\sigma^{n+4}} & \text{if } 1 \leq \sigma \leq \frac{1}{a} \\ \frac{\left\{ \begin{aligned} &1 - \frac{n(n+4)(1+a+a^2+\dots+a^{n+2})}{(n+2)(1+a+a^2+\dots+a^{n+3})\sigma} + \frac{n(n-1)(n+3)(n+4)(1+a+a^2+\dots+a^{n+1})}{2(n+1)(n+2)(1+a+a^2+\dots+a^{n+3})\sigma^2} \\ &\frac{(n+4)(n^4 + 2n^3 - 5n^2 - 6n + 4)}{2(n+1)(n+2)(1+a+a^2+\dots+a^{n+3})\sigma^{n+3}} \end{aligned} \right\}}{2(n+1)(n+2)(1+a+a^2+\dots+a^{n+3})\sigma^{n+3}} & \text{if } \sigma > \frac{1}{a} \end{cases}, \tag{D.4}$$

$$K = \frac{6\varphi(1+a+a^2+\dots+a^{n+3})}{(n+3)(n+4)} \left(\frac{h}{2}\right)^{n+1}; \quad \varphi = \frac{\pi(1+a+a^2)}{3} \left(\frac{h}{H}\right)^2. \tag{D.5,6}$$

(ii) Linear distributions of pores

For the first type of density function of linear probability distribution (given in Eq. (33)) of the pores in the circular tubes of the porous medium, one can obtain the analytical solutions for Darcy mean velocity of fluid flow, permeability and porosity as in Eqs. (D.7) – (D.9) respectively.

$$G(\sigma) = \begin{cases} 0 & \text{if } 0 \leq \sigma \leq 1 \\ \frac{\left\{ \begin{aligned} &4(n+1)(n+2)(n+4)\sigma^{n+5} - 4n(n+1)(n+3)(n+5)\sigma^{n+4} \\ &+ 2n(n-1)(n+2)(n+4)(n+5)\sigma^{n+3} - (n+4)(n+5)(n^4 + 2n^3 - 5n^2 - 6n + 4)\sigma^2 \\ &+ (n^6 + 10n^5 + 25n^4 - 22n^3 - 120n^2 - 42n + 64) \end{aligned} \right\}}{4(n+1)(n+2)(n+4)\sigma^{n+5}} & \text{if } \sigma > 1 \end{cases}, \tag{D.7}$$

$$K = \frac{8\varphi}{(n+3)(n+5)} \left(\frac{h}{2}\right)^{n+1}; \quad \varphi = \frac{\pi}{2} \left(\frac{h}{H}\right)^2. \tag{D.8,9}$$

When $\sigma \gg 1$, we get the expression for threshold level of pressure gradient as below:

$$\sigma_{pt} = \frac{n(n+3)(n+5)}{(n+2)(n+4)}. \tag{D.10}$$

For the second type of density function of the linear probability distribution (defined in Eq. (34)) of pores in the circular tube of the porous medium, the expressions for Darcy velocity, permeability and porosity can be obtained in the simplified form as in Eqs. (D. 11) – (D.13).

$$G(\sigma) = \begin{cases} 0 & \text{if } 0 \leq \sigma \leq 1 \\ \frac{\left\{ \begin{aligned} &4(n+1)(n+2)\sigma^{n+5} - 4n(n+1)(n+5)\sigma^{n+4} \\ &+ 2n(n-1)(n+4)(n+5)\sigma^{n+3} - (n+4)(n+5)(n^4 + 2n^3 - 5n^2 - 6n + 4)\sigma^2 \\ &+ 2(n+1)(n+5)(n^4 + 4n^3 - 5n^2 - 18n + 12)\sigma + (n+1)(n^5 + 8n^4 + 5n^3 - 70n^2 - 76n + 108) \end{aligned} \right\}}{4(n+1)(n+2)\sigma^{n+5}} & \text{if } \sigma > 1 \end{cases}, \tag{D.11}$$

$$SK = \frac{24\varphi}{(n+3)(n+4)(n+5)} \left(\frac{h}{2}\right)^{n+1}; \quad \varphi = \frac{\pi}{6} \left(\frac{h}{H}\right)^2. \tag{D.12,13}$$

When $\sigma \gg 1$, one can obtain the analytical expression for threshold pressure gradient as given below:

$$\sigma_{pt} = \frac{n(n+5)}{(n+2)}. \tag{D.14}$$

(iii) Quadratic distribution

When the pores of the flow region of the multi-pipes of the porous medium are modelled by the density function of the quadratic probability distribution (defined in Eq. (41)), the analytical expressions for Darcy velocity, flow medium’s permeability and porosity are obtained in the simplified form as in Eqs. (D.15) – (D.17):



$$G(\sigma) = \begin{cases} 0 & \text{if } 0 \leq \sigma \leq 1 \\ \left. \begin{aligned} & \left[\begin{aligned} & 12(n+1)(n+2)\sigma^{n+6} - 12n(n+1)(n+6)\sigma^{n+5} + 6n(n-1)(n+5)(n+6)\sigma^{n+4} \\ & - (n+4)(n+5)(n+6)(n^4 + 2n^3 - 5n^2 - 6n + 4)\sigma^3 \\ & + 3(n+1)(n+5)(n+6)(n^4 + 4n^3 - 5n^2 - 18n + 12)\sigma^2 \\ & - 3(n+1)(n+2)(n+6)(n^4 + 6n^3 - 3n^2 - 36n + 24)\sigma + (n+1)(n^5 + 8n^4 + 5n^3 - 70n^2 - 76n + 108) \end{aligned} \right] \\ & 12(n+1)(n+2)\sigma^{n+6} \end{aligned} \right\} & \text{if } \sigma > 1 \end{cases}, \quad (\text{D.15})$$

$$K = \frac{120 \varphi}{(n+3)(n+4)(n+5)(n+6)} \left(\frac{h}{2} \right)^{n+1}; \quad \varphi = \frac{\pi}{10} \left(\frac{h}{H} \right)^2 \quad (\text{D.16,17})$$

For quite large values of σ , $\sigma \gg 1$, Eq. (D.15) yields the expression for threshold level of pressure gradient as Eq. (D.18):

$$\sigma_{pt} = \frac{n(n+6)}{(n+2)}. \quad (\text{D.18})$$

References

- [1] Vafai, K., *Porous media: Applications in biological systems and biotechnology*, CRC Press: Taylor and Francis Group, 2011.
- [2] Chevalier T., Talon, L., Moving line model and avalanche statistics of Bingham fluid flow in porous media, *European Physical Journal E*, 38, 2015, 76 – 81.
- [3] Chen, M., Rossen, W., Yortsos, Y. C., The flow and displacement in porous media of fluids with yield stress, *Chemical Engineering: Science*, 60 2005, 4183–4202.
- [4] Ho, C. K., Webb, S. W., *Theory and Application of Transport in Porous Media*, Gas Transport, Springer, Netherlands, 2006.
- [5] J. Bleyer, J., Coussot, P., Breakage of non-Newtonian character in flow through porous medium: evidence from numerical simulation, *Physical Review E - American Physical Society*, 89, 2014, 063018.
- [6] Dullien, F. A. L., *Porous Media – Fluid Transport and pore structure*, Second Edition, Academic Press, MIT, U.S.A., 1992.
- [7] Heinemann, Z. E., *Fluid flow in porous media*, Textbook Ser. 1, 2003.
- [8] Chevalier, T., Rodts, S., Chateau, X., Chevalier, C., Coussot, P., Breaking of non-Newtonian character in flows through porous medium, *Physical Reviews Journal E*, 89, 2014, 023002.
- [9] Mehryan, S. A. M., Vaezi, M., Sheremet, M., Ghalambaz, M., Melting heat transfer of power-law-non-Newtonian phase change nano-enhanced n-octadecane-mesoporous silica (MPSiO₂), *Journal of Heat and Mass transfer*, 151, 2020, 119385.
- [10] Zadeh, S. M. H., Mehryan, S. A. M., Ghalambaz, M., Ghodrati, M., Young, J., Chamkha, A. J., Hybrid thermal performance enhancement of a circular latent heat storage system by utilizing partially filled copper foam and Cu/GO nano-additives, *Energy*, 213, 2020, 118761.
- [11] Ghalambaz, M., Sheremet, M., Mehryan, S. A. M., Kashkooli, F. M., Pop, I., Local thermal non-equilibrium analysis of conjugate free convection within a porous enclosure occupied with Ag-MgO hybrid nanofluid, *Journal of Thermal Analysis and Calorimetry*, 135, 2019, 1381 – 1398.
- [12] Ghalambaz, M., Zhang, J., Conjugate solid liquid-solid phase change heat transfer in heatsink filled with phase change material-metal foam, *International Journal of Heat and Mass Transfer*, 146, 2020, 118832.
- [13] Mehryan, S. A. M., Ghalambaz, M., Chamkha, A. J., Mohsenizadeh, Numerical study on natural convection of Ag-MgO hybrid/water nanofluid inside a porous enclosure: A local thermal non-equilibrium model, *Powder Technology*, 367, 2020, 443–445.
- [14] Coussot, P., Yield stress fluid flows: a review of experimental data, *Journal of Non-Newtonian Fluid Mechanics*, 211, 2014, 31–49.
- [15] Moller, B. P., Fall, A., Chikkadi, Y., Deres, D., Bonn, D., An attempt to categorize yield stress fluid behaviour, *Philosophical Transactions of Royal Society A*, 367, 2009, 5139–5155.
- [16] Kalogirou, A., Poyiadji, S., Georgiou, G. C., Incompressible Poiseuille flows of Newtonian liquids with pressure-dependent viscosity, *Journal of Non-Newtonian Fluid Mechanics*, 166, 2011, 413–419.
- [17] Zhu, H., Kim, Y. D., Kee, D. D., Non-Newtonian fluids with yield stress, *Journal of Non-Newtonian Fluid Mechanics*, 129, 2015, 177–181.
- [18] Pascal, H., Non-steady flow of non-Newtonian fluids through a porous medium, *International Journal of Engineering Science*, 21, 1983, 199–210.
- [19] Moller, P. C. F., Fall, A., Bonn, D., Origin of apparent viscosity in yield stress fluids below yielding, *EPL*, 87, 2009, 38004.
- [20] Balmforth, N. J., Frigaard, I. A., Ovarlez, G., Yielding to stress: recent developments in viscoplastic fluid mechanics, *Annual Reviews of Fluid Mechanics*, 46, 2014, 121–146.
- [21] Philippou, M., Kountouriotis, Z., Georgiou, G. C., Viscoplastic flow development in tubes and channels with wall slip, *Journal of Non-Newtonian Fluid Mechanics*, 234, 2016, 69–81.
- [22] Chevalier, T., Chevalier, C., Clain, X., Dupla, J. C., Canou, J. Rodts S., Coussot, P., Darcy's law for yield stress fluid flowing through a porous medium, *Journal of Non-Newtonian Fluid Mechanics*, 19, 2013, 57–66.
- [23] Balhoff, M. T., Rivera, D. S., Kwok, A., Mehmani, Y., Prodanovic, M., Numerical algorithms for network modeling of yield stress and other non-Newtonian fluids in porous media, *Transport in Porous Media*, 93, 2012, 363–379.
- [24] Papanastasiou, T. C., Flows of materials with yield stress, *Journal of Rheology*, 31, 1987, 385–404.
- [25] Nagarani, P., Sarojamma, G., Effect of body acceleration on pulsatile flow of Casson fluid through a mild stenosed artery, *Korea–Australia Rheology Journal*, 20, 2008, 189–196.
- [26] Sankar, D. S., Ismail, A. I. M., Effects of periodic body acceleration in blood flow through stenosed arteries – a theoretical model, *International Journal of Nonlinear Sciences and Numerical Simulations*, 11, 2010, 243 – 257.
- [27] Tu, C., Deville, M., Pulsatile flow of non-Newtonian fluids through arterial stenosis, *Journal of Biomechanics*, 29, 1996, 899–908.
- [28] Sankar, D. S., Two-phase non-linear model for blood flow in asymmetric and axisymmetric stenosed arteries, *International Journal of Non-Linear Mechanics*, 46, 2011, 296–305.
- [29] Mitsoulis, E., Abdali, S. S., Flow simulation of Herschel-Bulkley fluids through extrusion dies, *Canadian Journal of Chemical Engineering*, 71, 1993, 147–160.
- [30] Jaafar, N. A., Yatim, Y. M., Sankar, D. S., Effect of chemical reaction in solute dispersion in Herschel-Bulkley fluid flow with applications to blood flow, *Advances and Applications in Fluid Mechanics*, 20, 2017, 279–310.
- [31] Sabiri, N. E., Comiti, J., Pressure drop in non-Newtonian purely viscous fluid flow through porous media, *Chemical Engineering: Science*, 50, 1995, 1193–1201.
- [32] Lopez, X., Valvatne, P. H., Blunt, M. J., Predictive network modelling of single-phase non-Newtonian flow in porous media, *Journal of Colloid Interface Science*, 264, 2003, 256–265.
- [33] Darcy, H., *Les fontaines publiques de la ville de Dijon*, Victor Dalmont, Paris, 1856.
- [34] Prodanovic, M., Lindquist, W., Seright, R., Porous structure and fluid partitioning in polyethylene cores from 3D X-ray microtomographic imaging, *Journal of Colloid Interface Science*, 298, 2006, 282–297.
- [35] Sochi, T., Modelling the flow of yield-stress fluids in porous media, *Transport in Porous Media*, 85, 2010, 489–503.
- [36] Sanjari, A., Abbaszadah, M., Abassi, A., Lattice Boltzmann simulation of free convection in an inclined open ended cavity partially filled with fibrous porous media, *Journal of Porous Media*, 21, 2018, 1265–1281.
- [37] Abbaszadeh, M., Salehi, A., Abassi, A., Heat transfer enhancement in an asymmetrically heated channel partially filled with fibrous media – A



LBM approach, *Journal of Porous Media*, 18, 2015, 1201–1220.

[38] Oukhlef, A., Champmartin, S., Ambari, A., Yield stress fluids method to determine the pore size distribution of a porous medium, *Journal of Non-Newtonian Fluid Mechanics*, 204, 2014, 87–93.

[39] Chevalier, T., Chevalier, C., Clain, X., Dupla, J. C., Canou, J., Rodts, S., Coussot, P., Darcy's law for yield stress fluid flowing through a porous medium, *Journal of Non-Newtonian Fluid Mechanics*, 195, 2013, 57–66.

[40] Nash, S., Rees, D. A. S., The effect of microstructure on models for the flow of Bingham fluid in porous media: One dimensional flows, *Transport in Porous Media*, 116, 2017, 1073–1092.


[41] Sankar, D. S., Viswanathan, K. K., Mathematical analysis of Poiseuille flow of Casson fluid past porous medium, *Journal of Applied and Computational Mechanics*, 2019, DOI: 10.22055/JACM.2020.31961.1945.


[42] Purcell, W. R., Capillary pressures-their measurement using mercury and the calculation of permeability therefrom, *Petroleum Transport*, AIME, 186, 1949, 39–48.

[43] Falade, J. A., Ukaegbu, J. C., Egere, A. C., Adesanya, S. C., MHD oscillatory flow through a porous channel saturated with porous medium, *Alexandria Engineering Journal*, 56, 2017, 147–152.


[44] Chauhan, T. S., Chauhan, I. S., Shikka, S., Flow of viscous fluid through a porous circular pipe in presence of magnetic field, *Mathematica Aeterna*, 5, 2015, 395–402.


ORCID iD

D.S. Sankar  <https://orcid.org/0000-0002-9502-7841>

K.K. Viswanathan  <https://orcid.org/0000-0003-4470-4774>

Atulya K. Nagar  <https://orcid.org/0000-0001-5549-6435>

Nurul Aini Binti Jafaar  <https://orcid.org/0000-0003-4346-6786>

A. Vanav Kumar  <https://orcid.org/0000-0002-9502-7841>



© 2022 Shahid Chamran University of Ahvaz, Ahvaz, Iran. This article is an open access article distributed under the terms and conditions of the Creative Commons Attribution-NonCommercial 4.0 International (CC BY-NC 4.0 license) (<http://creativecommons.org/licenses/by-nc/4.0/>).

How to cite this article: Sankar D.S. et al., Theoretical Study on Poiseuille Flow of Herschel-Bulkley Fluid in Porous Media, *J. Appl. Comput. Mech.*, 8(4), 2022, 1246–1269. <https://doi.org/10.22055/JACM.2021.36921.2928>

Publisher's Note Shahid Chamran University of Ahvaz remains neutral with regard to jurisdictional claims in published maps and institutional affiliations.

